Gut microbiota impairment following graphene oxide exposure is associated to physiological alterations in Xenopus laevis tadpoles

Lauris Evariste, Florence Mouchet, Eric Pinelli, Emmanuel Flahaut, Laury Gauthier, Maialen Barret

Gut microbiota impairment following graphene oxide exposure is associated to physiological alterations in *Xenopus laevis* tadpoles

Lauris Evariste [a]*, Florence Mouchet [a], Eric Pinelli [a], Emmanuel Flahaut [b], Laury Gauthier [a], Maialen Barret [a]

[a] *Laboratoire Ecologie Fonctionnelle et Environnement, Université de Toulouse, CNRS, INPT, UPS, Toulouse, France*

[b] *CIRIMAT, Université de Toulouse, CNRS, INPT, UPS, UMR CNRS-UPS-INP N°5085, Université Toulouse 3 Paul Sabatier, Bât. CIRIMAT, 118 Route de Narbonne, 31062, Toulouse Cedex 9, France*

*Corresponding author: lauris.evariste@gmail.com phone: 0534323936

Abstract

Graphene-based nanomaterials such as graphene oxide (GO) possess unique properties triggering high expectations for the development of technological applications. Thus, GO is likely to be released in aquatic ecosystems. It is essential to evaluate its ecotoxicological potential to ensure a safe use of these nanomaterials. In amphibians, previous studies highlighted *X. laevis* tadpole growth inhibitions together with metabolic disturbances and genotoxic effects following GO exposure. As GO is known to exert bactericidal effects whereas the gut microbiota constitutes a compartment involved in host homeostasis regulation, it is important to determine if this microbial compartment constitutes a toxicological pathway involved in known GO-induced host physiological impairments. This study investigates the potential link between gut microbial communities and host physiological alterations. For this purpose, *X. laevis* tadpoles were exposed during 12 days to GO. Growth rate was monitored every 2 days and genotoxicity was assessed through enumeration of micronucleated erythrocytes. Genomic DNA was also extracted from the whole intestine to quantify gut bacteria and to analyze the community composition. GO exposure led to a dose dependent growth inhibition and genotoxic effects were detected following exposure to low doses. A transient decrease of the total bacteria was noticed

with a persistent shift in the gut microbiota structure in exposed animals. Genotoxic effects were associated to gut microbiota remodeling characterized by an increase of the relative abundance of *Bacteroides fragilis*. The growth inhibitory effects would be associated to a shift in the Firmicutes/Bacteroidetes ratio while metagenome inference suggested changes in metabolic pathways and upregulation of detoxification processes. This work indicates that the gut microbiota compartment is a biological compartment of interest as it is integrative of host physiological alterations and should be considered for ecotoxicological studies as structural or functional impairments could lead to later life host fitness loss.

Keywords: Amphibian; aquatic ecotoxicology; nanotoxicology; microbial ecology

Introduction

Benefiting from graphene-based nanomaterials (GBMs) properties, tremendous efforts are made for the development or the improvement of applications in a wide range of fields such as energy storage (Ali Tahir et al., 2016; Olabi et al., 2021), pollution remediation (Gopinath et al., 2021), medicine (Liu et al., 2013) or composite reinforcement (Ahmad et al., 2018). The improvement of production methods contributed to the increase of the annual production capacity of GBMs, including graphene oxide (GO), that are forecasted to be produced at industrial-scale within few years (Lin et al., 2019; Zhu et al., 2018). For these reasons, these nanomaterials are likely to be released in the environment at any stage of their life cycle (Ding et al., 2022; Freixa et al., 2018; Mottier et al., 2017), threatening ecosystems and associated wildlife, especially aquatic environments acting as a pollutant receptacle (Scown et al., 2010). Although no current information regarding environmental concentration of GBMs are available due to technological limitations (Goodwin et al., 2018), predicted environmental concentration of GO in aquatic ecosystem was estimated to be similar to those of carbon nanotubes ranging from 0.001 to 1,000 µg/L (De Marchi et al., 2018; Sun et al., 2016). Thus, carefully evaluating the ecotoxicological potential of GBMs is essential to ensure a safe use and a sustainable development of this nanotechnology.

Despite the knowledge gaps remaining concerning the evaluation of their ecotoxic potential (Fadeel et al., 2018; Jastrzębska and Olszyna, 2015), the data available from the literature indicate that GBMs can be accumulated through the trophic chain (Dong et al., 2018) and affect the physiology of organisms from different trophic levels (Evariste et al., 2020b; Montagner et al., 2016). Indeed, various toxic effects of GO towards aquatic organisms were observed, including physical membrane damages in bacteria (Mohammed et al., 2020; Sengupta et al., 2019), oxidative stress and shading effects in algae (Saxena et al., 2020; Yin et al., 2020), oxidative stress and motility impairment in the invertebrate *Daphnia magna* (Cano et al., 2017; Fekete-Kertész et al., 2020; Lv et al., 2018) or developmental

impairments, DNA damages, apoptosis, oxidative stress and immunotoxicity in zebrafish (M. Chen et al., 2016; Y. Chen et al., 2016; Souza et al., 2017).

In amphibian, previous studies highlighted that the growth of *Xenopus laevis* tadpoles was altered by exposure to GBMs (Mottier et al., 2016), including GO (Lagier et al., 2017). It was also highlighted that the tadpole growth inhibition was independent from a disruption of the thyroid pathway (Evariste et al., 2021b), while it was associated to a decrease of the fatty acids and triglyceride metabolism (Li et al., 2019). Intestinal accumulation of the nanomaterials favors direct contact with the gut microbiota which may be modulated by the nanomaterials and lead to host physiological alterations (Bantun et al., 2022). Indeed, while nutrients absorption and energy metabolism are known to rely on the gut microbiota homeostasis, it is of importance to determine if the alteration of the gut microbiota constitutes a toxicological pathway involved in GBMs-induced host physiological alterations. Emerging evidences indicate that the environmental pollution constitutes a major factor negatively influencing the composition and/or functioning of the host-associated microbial communities (Adamovsky et al., 2018; Duperron et al., 2020; Evariste et al., 2019a). However, this biological compartment is often unconsidered in ecotoxicology studies, focusing on host-centered biomarker measurements. In addition of playing a crucial role in the host physiological homeostasis, it was demonstrated that early-life alterations of the amphibian gut microbiome influence later life host fitness, through pathogen sensitivity increases or thermal tolerance impairments (Fontaine et al., 2022; Knutie et al., 2017). Thus, it is of crucial importance to consider both host and associated microbiota health in ecotoxicological studies as early life alteration of the gut microbiota could lead to threat for host population dynamic.

For this purpose, *X. laevis* tadpoles were exposed to increasing GO concentrations under similar conditions compared to the previously mentioned studies (Evariste et al., 2019b; Lagier et al., 2017), to determine the consequences towards gut microbial communities and the potential existing link between host physiological alterations and gut microbiota remodeling.

2. Materials and methods

2.1. *Xenopus laevis* breeding and exposure procedure

Sexually mature *Xenopus laevis* originated from our certified facilities (approval number A31113002). Spawning was induced by injection of 50 IU of pregnant mare's gonadotropin (PMSG 500; Intervet, France) in males and 750 IU of human chorionic gonadotropin (HCG; Organon, France) in females. The obtained fecundated eggs were bred in active charcoal filtered tap water at 22 ± 2°C and fed ad libitum with grinded aquarium fish food (TetraPhyll®, Tetra, Melle, Germany) until they reach stage 50 based on the Nieuwkoop & Faber development table (Nieuwkoop and Faber, 1958).

In accordance with the international standard ISO 21427-1 guidelines, groups of 20 larvae from stage 50 were exposed for 12 days under semi-static conditions to GO at 0; 0.05; 0.1; 1 or 10 mg/L. For comparison purpose, based on the specific surface area of the tested GO (Table 1) and according to previous works (Lagier et al., 2017; Mottier et al., 2016), the mass-concentration tested are equivalent to an exposure to a surface area per unit volume of 0; 0.0114; 0.0228; 0.228 and 2.28 m^2/L respectively. The experiment was conducted under natural dark/light cycle at 23.2 ± 0.2°C and feeding (TetraPhyll®, Tetra, Melle, Germany) as well as exposure media (294 mg/L $CaCl_2 \cdot 2H_2O$; 123.25 mg/L $MgSO_4 \cdot 7H2O$; 64.75 mg/L $NaHCO_3$; 5.75 mg/L KCl) were renewed daily to allow ad libitum feeding and water quality maintaining. Following 12 days of exposure, *X. laevis* larvae were anesthetized by bathing in 200 mg/L of MS222 solution in sodium bicarbonate prior samples collection. The whole experimental procedure was approved by an ethic committee (CEEA-073).

2.1. Graphene oxide characteristics, preparation of GO suspensions and behavior in exposure media

The graphene oxide used for this experiment was provided by Antolin Group and was prepared by oxidation of Grupo Antolin Carbon Nanofibers (GANF®) (Grupo Antolín, Burgos, Spain) using the Hummer's method (Hummers and Offeman, 1958; Lobato et al., 2016). The detailed characterization

of the GO batch used for this experiment was previously presented (Evariste et al., 2019b), demonstrating a non-significant amount of byproducts within the tested nanomaterials. The main characteristics of GO are summarized in Table 1.

For the experiment, GO was dispersed extemporaneously in deionized water to prepare a stock solution at 1 mg/mL. After 15 min sonication in ultrasonic bath (Bioblock 89863, typ 570 HF Freq 35 kHz), the stock solution was diluted to different concentrations in 20 mL of deionized water. Working solution of GO were sonicated during 2 minutes under same sonication conditions prior to exposure media contamination.

GO dispersion stability was evaluated using the UV-absorption properties of the nanomaterial, exhibiting an absorption peak at 235 nm (Johra et al., 2014). The experiment was conducted in triplicate at the single GO concentration of 10 mg/L due to detection limit constraints. Absorbance (235 nm) of the exposure media was measured in water column samples after 0; 10; 30; 60; 90; 120; 240; 420 and 1440 minutes, corresponding to the maximum duration prior media renewal, using CLARIOstar® microplate reader. GO concentrations were calculated using an absorbance-based calibration plot based on the optical density (OD) at 235nm, obtained after serial dilution of GO dispersions (Zhang et al., 2019). GO was quantified in the exposure media over time in absence as well as in presence of *X. laevis* tadpoles.

2.3. Growth measurement

In order to determine larval growth during the exposure, the length of the larvae was monitored since day 0 until day 12 every two days using ImageJ 1.49 software. Larval growth was calculated as a percentage of length increase since day 0. Normalized growth rate was determined as previously described (Mottier et al., 2016), using the following formula:

Normalized size (%) = $\left(\frac{(Ldt - MLd0)}{MLd0} \times 100\right) \times \left(\frac{100}{MLCdt}\right)$

With Ldt corresponding to the length of a larvae at the time of interest, MLd0 as the mean length of the larvae at day 0 from the exposure condition and MLCdt for the mean length of larvae from the negative control at the time of interest.

Intestinal growth was evaluated using similar calculations based on the intestinal weight instead of larval length.

2.4. Gut microbiota survey

Following anesthesia, ventral skin was incised to collect the whole intestine. Gut microbial community DNA was extracted from the whole larval intestine samples, snap frost in liquid nitrogen after 0(T0), 2 (T2) or 12 days (T12) of exposure (n = 5 per condition and per time). DNA extractions were performed using DNeasy PowerSoil kit (QIAGEN) as previously described for *X. laevis* gut samples (Evariste et al., 2020a).

Quantitative PCR (qPCR) targeting the universal 16S rRNA gene was used to measure the abundance of total intestinal bacteria. To provide a standard curve, tenfold factor dilution series of the gene ligated onto synthetic plasmid pEX-A128 (Eurofins Genomics, Belgium) was carried out. The reaction mixture (total volume = 10 µL) consisted of 5 µL of SsoAdvanced Universal SYBR Green Supermix (BioRad, United States), primer pairs (341-F CCTACGGGAGGCAGCAG / 534-R ATTACCGCGGCTGCTGGCA) and DNA template (diluted 100 times). Each reaction was run in triplicate in 96-well plates using a CFX96 Touch™ Real-Time PCR Detection System (BioRad, United States), using the following PCR protocol: 95°C for 130s, 35 cycles of 95°C for 5s, 60°C for 30s, 72°C for 10 minutes.

For 16S rRNA amplicon sequencing, the V4-V5 region of the gene was amplified from the whole intestine DNA extract using 515 F (5'-GTGYCAGCMGCCGCGGTA-3') / 928 R (5'-CCCCGYCAATTCMTTTRAGT-3') primer pair (Wang and Qian, 2009) and the following PCR protocol: 94°C for 120s, 30 cycles of 94°C for 60s, 65°C for 40s, 72°C for 10 minutes. The amplicon sequencing was performed by the Get_PlaGe platform (Genotoul, Toulouse, France) using an Illumina MiSeq (2x250 pb).

Microbiome bioinformatics were performed using QIIME 2 219.4 (Bolyen et al., 2019). Forward and reverse Illumina demultiplexed sequences were joined after import into QIIME2 prior denoising using DADA2 (Callahan et al., 2016). Based on the illumina primer used, trimming parameters were --p-trim-left-f 18 and --p-trim-left-r 19. According to interactive quality plots, truncation length parameter of DADA2 were -- p-trunc-len-f 220 and -- p-trunc-len-r 210. A total of 2,762,174 reads were obtained (minimum = 19,230, maximum = 61,452 and mean = 36,828.98). All amplicon sequence variants (ASVs) were aligned with mafft (Katoh et al., 2002) and a phylogenetic tree was built using FastTree (Price et al., 2009). Taxonomy was assigned to ASVs using the q2-feature-classifier (Bokulich et al., 2018), classify-sklearn naive Bayes taxonomy classifier against the Greengenes 13.8 99% OTUs reference sequences (McDonald et al., 2012).

To get insight at the species level of the most abundant ASV recovered, leading to a strong gut microbiota shift at T12 following exposure to low GO concentrations, a BLASTn search of the amplicon sequence was performed. The report suggested that the amplicon sequence produced significant alignment with Bacteroides fragilis (Accession: MN567591.1; Query covery: 100%; E-value: 2e-174; percentage identity: 97.07%).

PICRUSt2 (Phylogenetic Investigation of Communities by Reconstruction of Unobserved States) was used to predict functional gene content predictions based on 16S rRNA gene data (Douglas et al., 2020). The resulting abundance of KEGG (Kyoto Encyclopedia of Genes and Genomes) genes orthologues in each sample was categorized into biological pathways.

2.5. Micronucleated erythrocyte count and cell cycle analysis

Blood samples were collected through cardiac puncture. For micronuclei accounting, air dried blood smears are then fixed in methanol for 10 minutes prior staining with hematoxylin and eosin. Micronucleated erythrocytes are accounted over a total of 1000 cells (MNE ‰) using optical microscopy. For cell cycle analysis, blood sub-samples were fixed using cold ethanol (70% v/v) prior to perform analysis using Beckman Coulter Cytoflex flow cytometer (Beckman Coulter, USA). Cells were

stained using FxCycleTM PI/RNase Staining Solution (Life Technologies SAS) according to manufacturer's recommendations.

2.6. Statistical analysis

Graphs were generated and statistical analysis performed using the software GraphPad Prism 9.3.1. Data related to *X. laevis* physiological parameters such as growth rate or intestinal weights were analyzed using one-way analysis of variance (ANOVA) followed by Tukey test after verifying that the assumptions of normality and homogeneity of variance are met.

For microbiota survey, differences in the alpha diversity indexes and phyla relative abundances were analyzed for each sampling time by one-way analysis of variance (ANOVA) followed by Tukey test. Principal coordinates analysis (PCoA) plots were used to assess the variation between experimental conditions based on Bray-Curtis distances. Differences in beta-diversity were assessed *via* pairwise Permanova tests with 999 permutations. Intergroup taxa abundance differences were analyzed by the linear discriminant analysis (LDA) effect size (LEfSe) method (Segata et al., 2011). To conduct LEfSe analysis, the raw abundance of bacterial genera obtained from QIIME2 were exported on the Huttenhower Lab Galaxy Server (https://huttenhower.sph.harvard.edu/galaxy/root). For stringency, differentially abundant taxa that were statistically significant using an alpha of 0.05, and LDA score (log10) exceeding 3.0.

Differentially abundant pathways inferred using PiCRUSt2 2were evaluated using LEfSe analysis. Differentially abundant pathways were considered statistically significant using an alpha of 0.05, and LDA score (log10) exceeding 2.0.

Results from the micronucleus assay were statistically analyzed using McGill non-parametric test (Mcgill et al., 1978) on median values of each group of larvae as recommended in the standardized procedure ISO 21427-1. For cell-cycle data, after verifying the normal distribution of data, differences in cell-cycle phase distribution among conditions was evaluated using ANOVA followed by Tukey test.

3. Results

3.1. Exposure to GO affect larval growth

Using the calibration plot based on the optical absorbance at 235 nm of the GO dispersion used for our experiment (Figure 1A), GO concentration in the water column was determined to be 9.14 ± 0.34 mg/L immediately following exposure media contamination which is close to the nominal value of 10 mg/L expected. GO concentration in the water column decreased over time due to GO sedimentation, leading to a decreased GO concentration of 70.7 ± 5.4% after 420 minutes (Figure 1B). In presence of *X. laevis*, the water column is clear from GO only after 240 minutes (Figure 1B). Thus, the significantly lower area under the curve calculated from the GO concentration kinetic (T-test, $p < 0.001$) indicated that the presence of larvae in the exposure media is leading to a faster clearance of GO from the water column.

Monitoring of the larval growth parameters over the whole experiment indicated that GO exposure led to a time and dose-dependent alteration of the tadpole growth (Figure 2A). Growth inhibition is noticed following two days of exposure at the lowest dose of 0.05 mg/L (ANOVA, $p < 0.001$), while the growth of larvae exposed to the highest dose was decreased by 51.8 ± 17.7 % compared to the control group (Figure 2B). This effect is maintained over the whole experiment while growth alteration is less marked following 12 days of exposure as the growth of larvae exposed to 10 mg/L of GO is decreased by 20.7 ± 7.2 % compared to unexposed larvae (Figure 2C). Concomitant with the growth inhibition, a strong intestinal accumulation of GO is noticed in the gut of larvae exposed to any GO concentration after 2 days of exposure and up to the end of the experiment (Figure 2D).

Based on intestinal sample weights, larvae exposed to GBMs exhibited similar intestinal weight following 2 days of exposure to the different GO concentrations (ANOVA, $p = 0.732$) (Figure 2E) while only a significant decrease (ANOVA, $p = 0.018$) of intestinal weight is noticed after 12 days of exposure to GO at 10 mg/L, leading to a mean intestinal weight 37.8 ± 10.5 % lower compared to unexposed

larvae (Figure 2F). At the end of exposure, no developmental stage delay was observed as most of the tadpoles reached the NF stage 57 in all experimental conditions (ANOVA, $p = 0.093$) (Figure S1).

3.2. Exposure to GO transiently decrease the microbiota density

According to the 16S rRNA quantification of intestinal DNA extracts using qPCR, the results indicate that the amount of bacteria per mg of intestine remained constant over the experiment in larvae from the control group (ANOVA, $p = 0.814$) (Figure 3A). However, a transient decrease of 16S gene abundance is noticed following 2 days of exposure to the highest GO concentration (ANOVA, $p < 0.001$) prior recovering to similar values compared to the control group at T12 (ANOVA, $p = 0.666$) (Figure 3B,C).

3.3. Short term exposure to GO initiate a shift in the gut microbiota structure

Sequencing of the 16S rRNA V4-V5 region from gut DNA extracts allowed to explore for the consequences of an exposure to GO on the gut microbial communities structure and composition. While the gut microbial diversity indexes were similar between conditions prior to exposure media contamination (Figure S2), comparing the gut microbiome richness and diversity of unexposed tadpoles to the ones exposed during 2 days to increasing concentrations of GO indicated a significant increase of richness at the highest dose of exposure (ANOVA, $p = 0.035$) without influencing the Shannon index (Figure 4A, B). This suggest that the dominant species relative abundances from the gut microbiota are not impacted by the short duration of exposure to GO. However, based on Bray-Curtis distances, a significant increase of beta-diversity is noticed between the microbiota of larvae from the control group and those from larvae exposed to 0.05, 0.1 and 10 mg/L of GO while not following exposure to 1 mg/L (PERMANOVA, $p = 0.001$) (Figure 4C, D). PCoA plot and pairwise comparisons indicated that the microbiota shifted similarly in larvae exposed to 0.05 and 0.1 mg/L (Figure 4C).

At T2, the gut microbiota from control larvae is composed of three main phyla including Bacteroidetes, Firmicutes and Proteobacteria which relative abundances are respectively $54 \pm 6.4\%$, $25.5 \pm 5.2\%$ and $12.8 \pm 7.8\%$. In tadpoles exposed to GO, only larva exposed to 0.05 mg/L presented a microbiota

containing a significantly increased relative abundance of bacteria from the phylum Proteobacteria compared to the control group (ANOVA, $p = 0.005$). Otherwise, only slight nonsignificant modulations of others phyla relative abundances are observed (Figure 4E-I).

Analysis of differential taxa abundances using linear discriminant analysis (LDA) effect size (LEfSe) indicated that the exposure to the lowest GO concentrations led to an increased relative abundance of bacteria from the family *Cryomorphaceae* and genus *Rikenella* while the abundance of *Clostridiales* (order) decreased (Figure S3A). Following exposure to GO at 0.1 mg/L, larvae harbored a gut microbiota with increased proportion of bacteria from the genera *Rikenella* and *Acinetobacter* while bacteria from the family *Lachnospiraceae* decreased (Figure S3B). On contrary, none of the taxa found in the gut of larvae exposed to GO at 1 mg/L during 48 hours were differentially abundant compared to the control group. However, exposure to the highest GO concentration altered the abundance of bacteria from the family *Lachnospiraceae* and from the genus *Flectobacillus* while increased the proportion of *Anaerorhabdius furcosa* and family *Neisseriaceae* (Figure S3C).

3.4. Longer exposure duration to low or high GO concentrations differentially impair the gut microbiota

At the end of exposure (T12), a significant decrease of species richness is noticed in the gut microbiota of larvae exposed to 0.1 mg/L (ANOVA, $p = 0.0011$), while not in other conditions compared to the control group (Figure 5A). Considering the Shannon index, a significant and marked decrease of the index value is measured following 12 days of exposure to GO at 0.05 and 0.1 mg/L (ANOVA, $p < 0.001$) (Figure 5B). Based on Bray-Curtis dissimilarities analysis (Figure 5C, D), the results indicated that the gut bacterial communities of larvae exposed to GO at 0.05 and 0.1 mg/L were more dissimilar to the control group compared to larva exposed to the highest GO concentration, while larvae exposed to 1 mg/L exhibited a gut microbiota similar to the control group (PERMANOVA, $p = 0.001$).

As previously determined at T2, bacteria composing the gut microbiota of larvae from the control group at T12 belong to the phyla Bacteroidetes, Firmicutes and Proteobacteria with different relative

abundances, accounting respectively for 67.1 ± 5.2%, 11.6 ± 4.7% and 17.3 ± 8.2% of the whole bacterial populations (Figure 5E). At the phylum level, 12 days of exposure to GO led to a decrease of Bacteroidetes relative abundance following exposure to GO at 10 mg/L (ANOVA, $p < 0.001$), while bacteria from the phylum Firmicutes significantly increased in the gut of larvae following exposure to GO at 1 and 10 mg/L compared to larvae exposed to low GO concentrations (ANOVA, $p < 0.001$) (Figure 5F, G). Concomitantly, a significant increase of the relative abundance of bacteria from the phyla Proteobacteria is noticed following exposure to GO at 0.1 and 10 mg/L while the relative abundance of bacteria from the phyla Fusobacteria significantly decreased in the gut of larvae exposed to GO at 10 mg/L (Figure 5H, I). As a consequence of these changes, a dose-dependent increase of the Firmicutes/Bacteroidetes ratio is noticed (ANOVA, $p < 0.001$) (Figure 5J). Interestingly, at the genus level, the bacteria *Bacteroides fragilis* from the phylum Bacteroidetes became dominant following 12 days of exposure to GO at 0.05 and 0.1 mg/L, reaching up to 68.3% of the whole microbial community (ANOVA, $p < 0.001$). This increase of relative abundance benefited from the significant decrease of a bacteria from the genera Parabacteroides, belonging to the same phylum, after exposure to GO at low concentrations (Figure 5K). Such change in the relative abundance of these phyla can explain the previously described decrease of the Shannon index.

Determination of differential taxa abundances using linear discriminant analysis effect size (LEfSe) indicated that the phylum Proteobacteria was discriminant in the group of larvae exposed to GO at 0.05, 0.1 and 10 mg/L compared to the control group (Figure 6A-C). As for the LEfSe analysis performed at T2, none of the taxa allowed to discriminate the microbiome from the control larvae to the one of tadpoles exposed to GO at 1 mg/L for 12 days. However, more differentially abundant taxa were determined in animals exposed to GO at 10 mg/L compared to the control group (Figure 6C). Thus, the microbiome of larvae from the control group harbored a higher prevalence in bacteria from the genera *Bacteroides* and *Cetobacterium* (phylum Fusobacteria), while the abundance of bacteria from the family *Neisseriaceae* and *Lachnospiraceae* as well as genus *Rheinheimera* increased in larvae exposed to GO at 10 mg/L (LDA score [log10] > 4) (Figure 6 C, D).

3.5. Marked gut microbiota alterations following exposure to low GO concentrations are linked to genotoxic effects.

Exposure to low GO concentrations are associated to an increase in the relative abundance of the bacteria *Bacteroides fragilis* which is becoming dominant in the gut of tadpoles exposed to GO at 0.05 and 0.1 mg/L (Figure 7A). Under these conditions, the micronucleus assay revealed a significant increase of micronucleated erythrocytes following 12 days of exposure (Figure 7B). The absence of genotoxic effects in larvae exposed to the higher GO concentrations of 1 or 10 mg/L would be due to the decreased proportion of mitotic erythrocytes circulating in the tadpole bloodstream as indicated by the decreased proportion of cell populations in G2 phase (Table 2), decreasing the probability of micronuclei formation occurrence.

Interestingly, a significant linear correlation between the MNE occurrence and the relative abundance of Bacteroides fragilis can be found (Figure 7C) (Pearson, $r = 0.701$; $p < 0.001$). However, PCR analysis indicated no amplification of the targeted gene coding for the Bft from the gut microbiota samples, indicating that the *B. fragilis* strain recovered are not able to produce the enterotoxin.

3.6. Changes in gut microbiota structure following GO exposure predict functional alterations

PiCrust2 analysis showed evidences of predicted functions (KEGG genes collapsed at level 3) that are differentially abundant between the control and exposed groups, except after exposure to 1 mg/L of GO which is in accordance with the previously presented results indicating minimal gut microbiota modulations following exposure to this dose. Thus, LEfSe analysis identified 59, 42 and 65 pathways that differentiate the predicted functional profiles of the larvae exposed respectively to GO at 0.05, 0.1 and 10 mg/L from the control group. Among the tested conditions, 30 differentially abundant pathways compared to the control were shared following exposure to GO at 0.05 and 0.1 mg/L, suggesting closely-related toxicological effects (Figure S4A).

Under these conditions (0.05 and 0.1 mg/L), PICRUSt predicted functions indicated an increase of carbohydrate metabolism involving oxidative phosphorylation while glycolysis-related pathways are

downregulated as indicated by the decrease of pyruvate metabolism, pentose phosphate or glycolysis gluconeogenesis pathways compared to the control group (Figure S4B, C). The highest number of unique altered predicted function was found following exposure to the highest GO dose (Figure S4A). Under this exposure condition, the gut microbiota of exposed tadpoles exhibited upregulated pathways involved into bacterial motility and chemotaxis (Figure S4D). In addition, pathways related to the secretion system including ABC transporters, detoxification process involving cytochrome P450 and phosphotransferase system as well as naphthalene degradation are increased.

4. Discussion

4.1. Effects on larval growth

The bioavailability of GO, which conditions organism exposure in the environment, is influenced by its behavior in aquatic ecosystems (Ren et al., 2018). Thus, monitoring of GO behavior in the exposure media indicated a sedimentation of the nanomaterial over the time which was previously shown to be influenced by the interactions between GO surface functions and ions from the exposure media (Chowdhury et al., 2013). In the presence of larvae in the exposure media, the faster clearance of GO from the water column is due to larval filtration activity, leading to accumulation of the nanomaterial in the digestive tract as previously observed in amphibians (Lagier et al., 2017), zebrafish (Chen et al., 2021) and daphnids (Souza et al., 2018). Such exposure to GO is associated to larval growth inhibition within a similar magnitude compared to a previous study (Lagier et al., 2017). As the larvae from the group exposed to the highest dose exposed to GO during 12 days reached the size of unexposed larvae at day 8, the obtained results suggest a marked growth delay associated to high GO concentrations.

Over the metamorphosis process, the intestine of premetamorphic tadpoles consist in a simple thin tube which undergoes elongation, looping and rotation events (Bloom et al., 2013), as visible in unexposed larvae between T2 and T12. At the same time, gut complexity increases through crypt and villi structuration and shortening at climax (from stage 60) under the action of T3 hormone (Chalmers and Slack, 1998; Heimeier et al., 2010; Schreiber et al., 2005; Shi et al., 2001; Sterling et al., 2012).

Exposure to increasing GO concentrations did not led to the alteration of larval development as indicated by the similar NF stage 57 reached following 12 days of exposure to any GO concentration. While the stage 60 was not reached by any larvae at the end of the exposure, the gut shortening event taking place at this stage is unlikely to occur and the observed impairment of the intestinal maturation would be associated to GO exposure rather than due to a physiological process. Alteration of intestinal development were previously observed in zebrafish following GO exposure with no impact on fish growth (Zheng et al., 2019). However, in our study this effect is less marked compared to the larval growth inhibitory effects determined based on the larval length.

The larval growth inhibitory effects following exposure to increasing concentrations to GO are in line with previous studies performed using *X. laevis* as biological model (Lagier et al., 2017; Li et al., 2019). Such effects were shown to be associated to a decreased fatty acid and triglyceride metabolism as also observed in zebrafish exposed to GO, impairing their development as well as disturbing offspring metabolism (Hu et al., 2017; Li et al., 2019; Zhang et al., 2017). As metabolic disturbances were previously described in *X. laevis* tadpoles following exposure to GO at 1 mg/L, it is likely that the growth inhibition measured in our study imply similar pathways. The tadpole energy metabolism mainly relies on the gut microbiota metabolic capacities, providing energy substrates such as fatty acids for the host. Among fatty acids, short-chain fatty acids (SCFAs) including acetate, butyrate or propionate are metabolites produced through bacterial fermentation of dietary fibers in *X. laevis* intestine and were suggested to account for up to 20% of larval daily energy requirements (Koh et al., 2016; Pryor and Bjorndal, 2005; Scalvenzi et al., 2021). While energy metabolism is essential to ensure a proper larval development (Scott et al., 2007; Zhu et al., 2021), it is of importance to determine if the growth inhibition observed is associated to disturbances of the gut microbial communities, as many pollutants were previously described to alter intestinal microbial communities in aquatic organisms, impairing host fitness (Adamovsky et al., 2018; Evariste et al., 2019a; Sehnal et al., 2021).

4.2. Exposure to GO leads to alterations of the gut microbial community structure

It is now widely accepted that the host homeostasis depends on the gut microbiota health status (Lee and Hase, 2014; Sehnal et al., 2021). Thus, gut microbiota alteration following exposure to environmental pollution may lead to a loss of host fitness and affect the ability of a population to maintain (Evariste et al., 2019a). In addition, GO was previously described as a bactericidal nanomaterial and numerous studies described antibacterial activities through membrane impairment due to physical interactions, resulting in bacterial viability loss (Dizaj et al., 2015; Kumar et al., 2019; Tashan et al., 2019). Using the model bacteria *E. coli*, Liu and collaborators (Liu et al., 2011) demonstrated a decreased viability in a dose and time-dependent manner following exposure to GO at concentrations ranging from 5 to 80 µg/mL. Local intestinal accumulation of GO in the *X. laevis* intestine favor direct interactions with bacteria, leading to the observed effects. However, differential sensitivity to GBMs were shown depending on bacterial strains considered. Thereby, it was highlighted that membrane composition or bacterial shape also influences GBMs antimicrobial properties (Al-Thani et al., 2014; Sengupta et al., 2019; Tashan et al., 2019). As some studies indicated that GO may act as a promoter of bacterial biofilm formation (Guo et al., 2017; Ruiz et al., 2011), it is possible that the observed recovery in gut microbial density is associated to the presence of the nanomaterials in the gut that benefit to more tolerant bacteria colonizing this new ecological niche. Otherwise, one possible hypothesis is that GO accumulation in the intestine conduct to excretion of intestinal bacteria, explaining the transient abundance decrease. We then monitored the consequences of the exposure to GO on the gut microbial structures of the tadpoles.

The gut microbiota survey performed indicated that the tadpole intestine was mainly colonized by bacteria from the phyla Bacteroidetes, Proteobacteria and Firmicutes which is consistent with other studies in *Xenopus tropicalis* (Scalvenzi et al., 2021) or other vertebrates including mice or human (Colombo et al., 2015). In amphibians, gut microbiota remodeling is occurring over the metamorphosis process with food as one of the main driving factors (Kohl et al., 2014, 2013; Scalvenzi et al., 2021).

Indeed, dietary strategy changes within the metamorphosis switching from mainly herbivorous tadpoles to insectivorous froglets. Thus, the adaptative changes within the gut microbial communities allow the host to maintain energy intake in order to meet host metabolic requirements depending on the food available in different ecological niches (Bletz et al., 2016). Under our experimental conditions, tadpoles were maintained under constant abiotic parameters and artificial diets over a period which is not influenced by changes of feeding behavior. Thus, the effects observed towards microbial communities could be attributed to the GO exposure independently from host factors. The effects of GO exposure towards the gut microbiome was previously monitored using mice models (Chen et al., 2018; Li et al., 2018; Liu et al., 2021) or fish (Jia et al., 2019; Ma et al., 2016; Zheng et al., 2019), but to our knowledge, none using amphibians which physiology was previously shown to be affected by GO exposure (Evariste et al., 2019b; Lagier et al., 2017; Li et al., 2019).

The results from our study clearly indicated that short term exposure to GO (T2) initiates a shift of the gut microbial communities. Longer exposure duration is associated to strong gut microbiota disruption following exposure to low GO concentrations as indicated by the decrease of alpha diversity indexes and increase of Bray-Curtis distances, while the gut microbiota shifted differently and to a lower extent following exposure to higher GO concentrations. Nonlinear toxicological effects of nanoparticles were previously reported in the literature (Bell et al., 2013). Interestingly, a study performed in mice orally exposed to pristine graphene indicated that an exposure to a dose of 1µg/d exerted stronger deleterious influence on the gut microbiota of mice compared to higher concentration of 10 or 100 µg/d (Xie et al., 2016). The authors suggested that the differential effects could be associated to differences of aggregation states of the nanomaterials between high and low graphene doses. Indeed, it was previously described that an increased aggregation state reduces GBMs antibacterial activities (Hegab et al., 2016; Liu et al., 2011). In addition, it was indicated that GBMs aggregation increases at high concentration and that physicochemical parameters of the environment such as pH or ion concentrations, which are also likely to fluctuate within the digestive tract microenvironment, may also influence aggregation states (Gao et al., 2022; Suter and Coveney, 2021). Thus, it is likely that the

more marked adverse effects on microbial communities occurring in the present study would be due to the differences of aggregation states in the gut of tadpoles exposed to low concentrations compared to higher concentrations.

Despite that other physicochemical characteristics of the GBMs such as the oxidation degree or lateral size dimension were previously shown to influence their antimicrobial properties (Perreault et al., 2015; Zou et al., 2016), a similar trend is noticed between several studies focusing on the effects of GO on the gut microbiota of other species (Jia et al., 2019; Liu et al., 2021; Zheng et al., 2019), leading to a decrease of the relative abundance of bacteria from the phylum Bacteroidetes that is consistent with the present results. Similar effects were also observed in various microbial consortia exposed to GBMs such as in soil (Du et al., 2015), biofilms (Evariste et al., 2021a) or swine manure (Zhang et al., 2017), suggesting an overall higher susceptibility of most of bacteria from this phylum to GO. In amphibians, tadpole's energy metabolism during the pro-metamorphosis stages mainly relies on carbohydrate and lipid metabolism which are essential to ensure metamorphosis events (Zhu et al., 2020, 2019). While gut bacteria from the phylum Bacteroidetes were shown to be involved in the polysaccharides and carbohydrate degradation (Gibiino et al., 2018), the decreased Bacteroidetes relative abundance in the gut of exposed larvae might be associated to an impairment of these metabolic pathways as previously observed in *X. laevis* tadpoles exposed to GO at concentrations up to 1 mg/L (Li et al., 2019), leading to larval growth inhibition. This hypothesis could be suggested by the significant linear correlation found between the larval growth rate and the relative abundance of bacteria from the phylum Bacteroidetes (Pearson correlation, $r = 0.496$, $p = 0.011$).

It is worth to note that the exposure to GO also influence the relative abundance of gut bacteria from the phylum *Fusobacteria*, leading to a decreased proportion compared to the control group following exposure to GO at the highest concentration. Previous studies suggested that this phylum was involved in priming the immune system during amphibian early-life stages. Indeed, a lower *Fusobacteria* abundance or gut richness during early-life stages predicted an increased host susceptibility to

458 pathogens during later life at adulthood (Knutie et al., 2018, 2017). Thus, even if it is remaining to be
459 evaluated, early-life exposure to GO might be likely to have deleterious consequences for the host
460 through an alteration of its immune system maturation.

461 Concomitant with the decrease of Bacteroidetes relative abundance, an increase of the Firmicutes
462 proportion is noticed. Thus, exposure to GO led to changes in niche partitioning between these two
463 major phyla leading to an increase of the F/B ratio. An increase of Firmicutes/Bacteroidetes ratio was
464 previously observed in mice exposed to GO (Chen et al., 2018; Liu et al., 2021). These phyla were
465 suggested to possess distinct and complementary metabolic capacities within the gut microbial
466 communities and imbalance in this ratio is generally associated to metabolic disorders in humans such
467 as obesity (Ley et al., 2006a, 2006b). In mice model, the increase of F/B ratio can be induced by energy-
468 rich diet consumption, leading to disturbances of the gut metabolism through alteration of the SCFA
469 production profile which is associated to the occurrence of metabolic syndromes (Woting and Blaut,
470 2016). Consistent with this, it was observed that rice frogs, Fejervarya *limnocharis,* living in farmland
471 environments characterized by an altered diet composition exhibited a higher F/B ratio and increased
472 Proteobacteria compared to populations from natural environments benefiting from more diverse
473 food sources (Chang et al., 2016). Otherwise, exposure of *X. tropicalis* to antibiotics was indicated to
474 alter the composition of adult frog gut flora, leading to an increase in the F/B ratio without establishing
475 link with host-related endpoints (Lin et al., 2022). As Firmicutes are suggested to be involved in energy
476 harvesting (Krajmalnik-Brown et al., 2012; Ley et al., 2006b), changes in their relative abundance may
477 alter the production of gut microbial metabolites involved in multiple host metabolic pathways,
478 unbalancing energy intake and storage, affecting larval metamorphosis and later life fitness (Crespi
479 and Warne, 2013; Zhu et al., 2019). Indeed, even if the tadpoles complete their metamorphosis, size
480 at metamorphosis is correlated to a better survival of the adults and locomotive performances (Székely
481 et al., 2020).

482

4.3. Genotoxic effects detected in the host do not seem to be mediated by the gut microbiota

Consistent with our results, it was previously indicated that exposure to low GO concentrations induce genotoxic effects in amphibians (Evariste et al., 2020b, 2019b). The later study was performed using similar nanomaterials and deciphered the involvement of oxygen-containing surface functions of GO in genotoxic effects towards *X. laevis*. (Evariste et al., 2019b). Importantly, the bacteria *Bacteroides fragilis* which is becoming dominant in the gut of tadpoles exposed to GO at 0.05 and 0.1 mg/L. Enterotoxigenic strains of B. fragilis are known to causes colitis and promote colon tumorigenesis through the induction of genotoxic effects associated to the production of the bacteroides fragilis toxin (bft) (Chung et al., 2018; Goodwin et al., 2011). Thus, a particular attention was paid to the occurrence of micronucleated erythrocytes in tadpoles following 12 days of exposure, in order to allow micronuclei formation (Fernandez et al., 1993), in connection with the increased relative abundance of *Bacteroides fragilis.* The presence of *bft* gene in the gut of larvae exposed to the different GO concentrations was evaluated using PCR (Pantosti et al., 1997) to determine if the production of toxins within the gut could contribute to the occurrence of genotoxic effects in the host. However, no amplification of the targeted gene coding for the Bft resulted from PCR analysis of the gut microbiota samples, indicating that the *B. fragilis* strain are not able to produce the enterotoxin. Thus, even if the link between diversity loss and host physiological impairment is being remaining to be understood, it is likely that the genotoxic effects are mediated by oxidative stress induced by GO as previously suggested, with no involvement of gut pathobionts (Evariste et al., 2019b).

4.4. Functional predictions suggest that changes in gut microbiota structure are associated to metabolic alterations

To gain insight into the potential functional adverse effects of GO exposure associated to the alterations of the microbial communities, functional pathways were predicted using PiCrust2 analysis on 16S amplicon sequencing data. The algorithm predictions suggested that a shift in energy metabolism occurred in tadpoles exposed to low GO concentrations through an increase of

carbohydrate metabolism involving oxidative phosphorylation while glycolysis-related pathways are downregulated as indicated by the decrease of pyruvate metabolism, pentose phosphate or glycolysis gluconeogenesis pathways compared to the control group. Glycolysis and oxidative phosphorylation are two major metabolic pathways to provide energy. However, the oxidative phosphorylation process inevitably results in the generation of free radicals that can lead to DNA damages compared to glycolysis which limit oxidative damages (Brace et al., 2016). This is consistent with the previous studies revealing that *X. laevis* tadpoles exposure to similar GO dose (0.1 mg/L) was leading to the induction of oxidative stress and genotoxic effects (Evariste et al., 2019b).

On contrary, exposure to high GO doses led to different effects as indicated by the upregulation of pathways involved into bacterial motility and chemotaxis. Even though we were not able to confirm an increase of gut microbiota flagellin levels using human embryonic kidney (HEK)-Blue-mTLR5 cells as previously described (Chassaing et al., 2014) (data not shown) probably due to graphene capacities to adsorb bacterial flagellar components (Tegou et al., 2016; Zhang et al., 2020), bacterial motility increase bacteria-host epithelium interactions, leading to deleterious effects for the host through the promotion of pro-inflammatory effects mediated by toll-like receptors 5 (TLR5) (Miclotte et al., 2020; Wiles et al., 2020). In addition, increased xenobiotic detoxification capacities are suggested under this condition by the increase of pathways related to secretion system including ABC transporters which are involved in efflux of products across the cell membrane (Davidson and Chen, 2004) and detoxification process as indicated by the increase of cytochrome P450 activity and phosphotransferase system which are involved in anti-stress responses (Cryle et al., 2003; Peng et al., 2017). Interestingly, the pathway related to naphthalene degradation is also increased. As naphthalene-degrading bacteria isolated from graphite mine were previously shown to degrade GO (Liu et al., 2015), this suggest that GO-induced selective pressure, drive a shift in the gut microbiota which is associated to improved detoxification and GO degradation capacities. However, this seems to be leading to decreased metabolic capacities as indicated by the decrease of glucose-related metabolic pathways, amino acid metabolism, fatty acid biosynthesis which together, contribute to the host

energy metabolism. Such alteration of metabolic pathways were previously shown to be induced by GO exposure in *X. laevis* while essential for larval development and might lead to the observed larval growth inhibition (Li et al., 2019; Zhu et al., 2021). Even if the Picrust analysis display more accurate results from gut microbiota data compared to other microbial compartment, there is a need to be cautious with the results from our study based on non-human biological models, which shown lower performances due to the intrinsic limits of the method (Sun et al., 2020). Thus, even if the obtained results propose interesting pathways which might be involved in host physiological alterations, there is a need to confirm these results in further studies using shotgun sequencing analysis (Ranjan et al., 2016).

5. Conclusion

The results obtained in this study demonstrate that *X. laevis* larvae exposure to GO leads to gut microbiota alterations which are linked to host physiological impairments including DNA damages and growth inhibition. Based on the obtained results and the data available from the literature, the larval growth impairment associated to gut microbiota structure disruption constitute two risk factors which could conduct to later-life host fitness loss through potentially decreased survival of individuals, impairment of immune performances or decrease of thermal tolerance. Thus, even if this is remaining to be determined in future study, the marked effects of GO towards gut microbial communities, even at environmentally relevant concentrations could be deleterious for amphibian population dynamic. Overall, this study highlights that the monitoring of the gut microbiota status in response to GBMs constitute a good integrative marker of the overall host physiological alterations.

Declaration of competing interest

The authors declare that they have no known competing financial interests or personal relationships that could have appeared to influence the work reported in this paper.

Acknowledgment

The authors thank the European Union's Horizon 2020 research and innovation program under grant agreement No 696656 & 785219 (Flagship). Thanks to the Dr. Laura Lagier for technical support in the analysis of GO concentration in the exposure media. We would like to thanks the ENteRisk Team from the Food Toxicology Center of Toulouse (INRAE) for its expertise and involvement in the assessment of gut flagellin levels which were evaluated during the experiments. The authors are grateful to the Genotoul bioinformatics platform Toulouse Midi-Pyrenees and the Sigenae group for providing computing and storage resources.

References

Adamovsky, O., Buerger, A.N., Wormington, A.M., Ector, N., Griffitt, R.J., Bisesi Jr., J.H., Martyniuk, C.J., 2018. The gut microbiome and aquatic toxicology: An emerging concept for environmental health. Environmental Toxicology and Chemistry 37, 2758–2775. https://doi.org/10.1002/etc.4249

Ahmad, H., Fan, M., Hui, D., 2018. Graphene oxide incorporated functional materials: A review. Composites Part B: Engineering 145, 270–280. https://doi.org/10.1016/j.compositesb.2018.02.006

Ali Tahir, A., Ullah, H., Sudhagar, P., Asri Mat Teridi, M., Devadoss, A., Sundaram, S., 2016. The application of graphene and Its derivatives to energy conversion, storage, and environmental and biosensing devices. The Chemical Record 16, 1591–1634. https://doi.org/10.1002/tcr.201500279

Al-Thani, R.F., Patan, N.K., Al-Maadeed, M.A., 2014. Graphene oxide as antimicrobial against two gram-positive and two gram-negative bacteria in addition to one fungus. OnLine Journal of Biological Sciences 14, 230–239. https://doi.org/10.3844/ojbsci.2014.230.239

Bantun, F., Singh, R., Alkhanani, M.F., Almalki, A.H., Alshammary, F., Khan, S., Haque, S., Srivastava, M., 2022. Gut microbiome interactions with graphene based nanomaterials: Challenges and opportunities. Science of The Total Environment 830, 154789. https://doi.org/10.1016/j.scitotenv.2022.154789

Bell, I.R., Ives, J.A., Jonas, W.B., 2013. Nonlinear Effects of Nanoparticles: Biological Variability From Hormetic Doses, Small Particle Sizes, and Dynamic Adaptive Interactions. Dose Response 12, 202–232. https://doi.org/10.2203/dose-response.13-025.Bell

Bletz, M.C., Goedbloed, D.J., Sanchez, E., Reinhardt, T., Tebbe, C.C., Bhuju, S., Geffers, R., Jarek, M., Vences, M., Steinfartz, S., 2016. Amphibian gut microbiota shifts differentially in community structure but converges on habitat-specific predicted functions. Nature Communications 7, 13699. https://doi.org/10.1038/ncomms13699

Bloom, S., Ledon-Rettig, C., Infante, C., Everly, A., Hanken, J., Nascone-Yoder, N., 2013. Developmental origins of novel gut morphology in frogs. Evol Dev 15, 10.1111/ede.12035. https://doi.org/10.1111/ede.12035

Bokulich, N.A., Kaehler, B.D., Rideout, J.R., Dillon, M., Bolyen, E., Knight, R., Huttley, G.A., Gregory Caporaso, J., 2018. Optimizing taxonomic classification of marker-gene amplicon sequences with QIIME 2's q2-feature-classifier plugin. Microbiome 6, 90. https://doi.org/10.1186/s40168-018-0470-z

Bolyen, E., Rideout, J.R., Dillon, M.R., Bokulich, N.A., Abnet, C.C., Al-Ghalith, G.A., Alexander, H., Alm, E.J., Arumugam, M., Asnicar, F., Bai, Y., Bisanz, J.E., Bittinger, K., Brejnrod, A., Brislawn, C.J., Brown, C.T., Callahan, B.J., Caraballo-Rodríguez, A.M., Chase, J., Cope, E.K., Da Silva, R., Diener, C., Dorrestein, P.C., Douglas, G.M., Durall, D.M., Duvallet, C., Edwardson, C.F., Ernst, M., Estaki, M., Fouquier, J., Gauglitz, J.M., Gibbons, S.M., Gibson, D.L., Gonzalez, A., Gorlick, K., Guo, J., Hillmann, B., Holmes, S., Holste, H., Huttenhower, C., Huttley, G.A., Janssen, S., Jarmusch, A.K., Jiang, L., Kaehler, B.D., Kang, K.B., Keefe, C.R., Keim, P., Kelley, S.T., Knights, D., Koester, I., Kosciolek, T., Kreps, J., Langille, M.G.I., Lee, J., Ley, R., Liu, Y.-X., Loftfield, E., Lozupone, C., Maher, M., Marotz, C., Martin, B.D., McDonald, D., McIver, L.J., Melnik, A.V., Metcalf, J.L., Morgan, S.C., Morton, J.T., Naimey, A.T., Navas-Molina, J.A., Nothias, L.F., Orchanian, S.B., Pearson, T., Peoples, S.L., Petras, D., Preuss, M.L., Pruesse, E., Rasmussen, L.B., Rivers, A., Robeson, M.S., Rosenthal, P., Segata, N., Shaffer, M., Shiffer, A., Sinha, R., Song, S.J., Spear, J.R., Swafford, A.D., Thompson, L.R., Torres, P.J., Trinh, P., Tripathi, A., Turnbaugh, P.J., Ul-Hasan, S., van der Hooft, J.J.J., Vargas, F., Vázquez-Baeza, Y., Vogtmann, E., von Hippel, M., Walters, W., Wan, Y., Wang, M., Warren, J., Weber, K.C., Williamson, C.H.D., Willis, A.D., Xu, Z.Z., Zaneveld, J.R., Zhang, Y., Zhu, Q., Knight, R., Caporaso, J.G., 2019. Reproducible, interactive, scalable and extensible microbiome data science using QIIME 2. Nat Biotechnol 37, 852–857. https://doi.org/10.1038/s41587-019-0209-9

Brace, L.E., Vose, S.C., Stanya, K., Gathungu, R.M., Marur, V.R., Longchamp, A., Treviño-Villarreal, H., Mejia, P., Vargas, D., Inouye, K., Bronson, R.T., Lee, C.-H., Neilan, E., Kristal, B.S., Mitchell, J.R., 2016. Increased oxidative phosphorylation in response to acute and chronic DNA damage. npj Aging Mech Dis 2, 1–11. https://doi.org/10.1038/npjamd.2016.22

Callahan, B.J., McMurdie, P.J., Rosen, M.J., Han, A.W., Johnson, A.J.A., Holmes, S.P., 2016. DADA2: High resolution sample inference from Illumina amplicon data. Nat Methods 13, 581–583. https://doi.org/10.1038/nmeth.3869

Cano, A.M., Maul, J.D., Saed, M., Shah, S.A., Green, M.J., Cañas-Carrell, J.E., 2017. Bioaccumulation, stress, and swimming impairment in Daphnia magna exposed to multiwalled carbon nanotubes, graphene, and graphene oxide. Environmental Toxicology and Chemistry 36, 2199–2204. https://doi.org/10.1002/etc.3754

Chalmers, A.D., Slack, J.M., 1998. Development of the gut in Xenopus laevis. Dev. Dyn. 212, 509–521. https://doi.org/10.1002/(SICI)1097-0177(199808)212:4<509::AID-AJA4>3.0.CO;2-L

Chang, C.-W., Huang, B.-H., Lin, S.-M., Huang, C.-L., Liao, P.-C., 2016. Changes of diet and dominant intestinal microbes in farmland frogs. BMC Microbiology 16. https://doi.org/10.1186/s12866-016-0660-4

Chassaing, B., Koren, O., Carvalho, F.A., Ley, R.E., Gewirtz, A.T., 2014. AIEC pathobiont instigates chronic colitis in susceptible hosts by altering microbiota composition. Gut 63, 1069–1080. https://doi.org/10.1136/gutjnl-2013-304909

Chen, H., Zhao, R., Wang, B., Zheng, L., Ouyang, H., Wang, H., Zhou, X., Zhang, D., Chai, Z., Zhao, Y., Feng, W., 2018. Acute Oral Administration of Single-Walled Carbon Nanotubes Increases Intestinal Permeability and Inflammatory Responses: Association with the Changes in Gut Microbiota in Mice. Adv Healthc Mater 7, e1701313. https://doi.org/10.1002/adhm.201701313

Chen, M., Yin, J., Liang, Y., Yuan, S., Wang, F., Song, M., Wang, H., 2016. Oxidative stress and immunotoxicity induced by graphene oxide in zebrafish. Aquatic Toxicology 174, 54–60. https://doi.org/10.1016/j.aquatox.2016.02.015

Chen, P., Yang, J., Xiao, B., Zhang, Y., Liu, S., Zhu, L., 2021. Mechanisms for the impacts of graphene oxide on the developmental toxicity and endocrine disruption induced by bisphenol A on zebrafish larvae. Journal of Hazardous Materials 408, 124867. https://doi.org/10.1016/j.jhazmat.2020.124867

Chen, Y., Hu, X., Sun, J., Zhou, Q., 2016. Specific nanotoxicity of graphene oxide during zebrafish embryogenesis. Nanotoxicology 10, 42–52. https://doi.org/10.3109/17435390.2015.1005032

Chowdhury, I., Duch, M.C., Mansukhani, N.D., Hersam, M.C., Bouchard, D., 2013. Colloidal properties and stability of graphene oxide nanomaterials in the aquatic environment. Environmental Science & Technology 47, 6288–6296. https://doi.org/10.1021/es400483k

Chung, L., Thiele Orberg, E., Geis, A.L., Chan, J.L., Fu, K., DeStefano Shields, C.E., Dejea, C.M., Fathi, P., Chen, J., Finard, B.B., Tam, A.J., McAllister, F., Fan, H., Wu, X., Ganguly, S., Lebid, A., Metz, P., Van Meerbeke, S.W., Huso, D.L., Wick, E.C., Pardoll, D.M., Wan, F., Wu, S., Sears, C.L., Housseau, F., 2018. Bacteroides fragilis Toxin Coordinates a Pro-carcinogenic Inflammatory Cascade via Targeting of Colonic Epithelial Cells. Cell Host & Microbe 23, 203-214.e5. https://doi.org/10.1016/j.chom.2018.01.007

Colombo, B.M., Scalvenzi, T., Benlamara, S., Pollet, N., 2015. Microbiota and Mucosal Immunity in Amphibians. Frontiers in Immunology 6. https://doi.org/10.3389/fimmu.2015.00111

Crespi, E.J., Warne, R.W., 2013. Environmental Conditions Experienced During the Tadpole Stage Alter Post-metamorphic Glucocorticoid Response to Stress in an Amphibian. Integrative and Comparative Biology 53, 989–1001. https://doi.org/10.1093/icb/ict087

Cryle, M.J., Stok, J.E., Voss, J.J.D., 2003. Reactions Catalyzed by Bacterial Cytochromes P450. Aust. J. Chem. 56, 749–762. https://doi.org/10.1071/ch03040

Davidson, A.L., Chen, J., 2004. ATP-Binding Cassette Transporters in Bacteria. Annual Review of Biochemistry 73, 241–268. https://doi.org/10.1146/annurev.biochem.73.011303.073626

De Marchi, L., Pretti, C., Gabriel, B., Marques, P.A.A.P., Freitas, R., Neto, V., 2018. An overview of graphene materials: Properties, applications and toxicity on aquatic environments. Science of The Total Environment 631–632, 1440–1456. https://doi.org/10.1016/j.scitotenv.2018.03.132

Ding, X., Pu, Y., Tang, M., Zhang, T., 2022. Environmental and health effects of graphene-family nanomaterials: Potential release pathways, transformation, environmental fate and health risks. Nano Today 42, 101379. https://doi.org/10.1016/j.nantod.2022.101379

Dizaj, S.M., Mennati, A., Jafari, S., Khezri, K., Adibkia, K., 2015. Antimicrobial activity of carbon-based nanoparticles. Advanced pharmaceutical bulletin 5, 19.

Dong, S., Xia, T., Yang, Y., Lin, S., Mao, L., 2018. Bioaccumulation of 14C-Labeled Graphene in an Aquatic Food Chain through Direct Uptake or Trophic Transfer. Environ. Sci. Technol. 52, 541–549. https://doi.org/10.1021/acs.est.7b04339

Douglas, G.M., Maffei, V.J., Zaneveld, J.R., Yurgel, S.N., Brown, J.R., Taylor, C.M., Huttenhower, C., Langille, M.G.I., 2020. PICRUSt2 for prediction of metagenome functions. Nat Biotechnol 38, 685–688. https://doi.org/10.1038/s41587-020-0548-6

Du, J., Hu, X., Zhou, Q., 2015. Graphene oxide regulates the bacterial community and exhibits property changes in soil. RSC Advances 5, 27009–27017. https://doi.org/10.1039/C5RA01045D

Duperron, S., Halary, S., Gallet, A., Marie, B., 2020. Microbiome-Aware Ecotoxicology of Organisms: Relevance, Pitfalls, and Challenges. Frontiers in Public Health 8.

Evariste, L., Barret, M., Mottier, A., Mouchet, F., Gauthier, L., Pinelli, E., 2019a. Gut microbiota of aquatic organisms: A key endpoint for ecotoxicological studies. Environmental Pollution 248, 989–999. https://doi.org/10.1016/j.envpol.2019.02.101

Evariste, L., Braylé, P., Mouchet, F., Silvestre, J., Gauthier, L., Flahaut, E., Pinelli, E., Barret, M., 2021a. Graphene-Based Nanomaterials Modulate Internal Biofilm Interactions and Microbial Diversity. Front. Microbiol. 12. https://doi.org/10.3389/fmicb.2021.623853

Evariste, L., Flahaut, E., Baratange, C., Barret, M., Mouchet, F., PINELLI, E., Galibert, A.M., Soula, B., GAUTHIER, L., 2020a. Ecotoxicological assessment of commercial Boron Nitride Nanotubes towards *Xenopus laevis* tadpoles and host-associated gut microbiota. Nanotoxicology. https://doi.org/10.1080/17435390.2020.1839137

Evariste, L., Lagier, L., Gonzalez, P., Mottier, A., Mouchet, F., Cadarsi, S., Lonchambon, P., Daffe, G., Chimowa, G., Sarrieu, C., Ompraret, E., Galibert, A.-M., Ghimbeu, C.M., Pinelli, E., Flahaut, E., Gauthier, L., 2019b. Thermal reduction of graphene oxide mitigates its in vivo genotoxicity toward Xenopus laevis tadpoles. Nanomaterials 9, 584. https://doi.org/10.3390/nano9040584

Evariste, L., Mottier, A., Lagier, L., Cadarsi, S., Barret, M., Sarrieu, C., Soula, B., Mouchet, F., Flahaut, E., Pinelli, E., Gauthier, L., 2020b. Assessment of graphene oxide ecotoxicity at several trophic

levels using aquatic microcosms. Carbon 156, 261–271. https://doi.org/10.1016/j.carbon.2019.09.051
Evariste, L., Mottier, A., Pinelli, E., Flahaut, E., Gauthier, L., Mouchet, F., 2021b. Graphene oxide and reduced graphene oxide promote the effects of exogenous T3 thyroid hormone in the amphibian Xenopus laevis. Chemosphere 281, 130901. https://doi.org/10.1016/j.chemosphere.2021.130901
Fadeel, B., Bussy, C., Merino, S., Vázquez, E., Flahaut, E., Mouchet, F., Evariste, L., Gauthier, L., Koivisto, A.J., Vogel, U., Martín, C., Delogu, L.G., Buerki-Thurnherr, T., Wick, P., Beloin-Saint-Pierre, D., Hischier, R., Pelin, M., Candotto Carniel, F., Tretiach, M., Cesca, F., Benfenati, F., Scaini, D., Ballerini, L., Kostarelos, K., Prato, M., Bianco, A., 2018. Safety assessment of graphene-based materials: Focus on human health and the environment. ACS Nano 12, 10582–10620. https://doi.org/10.1021/acsnano.8b04758
Fekete-Kertész, I., László, K., Terebesi, C., Gyarmati, B.S., Farah, S., Márton, R., Molnár, M., 2020. Ecotoxicity Assessment of Graphene Oxide by Daphnia magna through a Multimarker Approach from the Molecular to the Physiological Level including Behavioral Changes. Nanomaterials 10, 2048. https://doi.org/10.3390/nano10102048
Fernandez, M., L'Haridon, J., Gauthier, L., Zoll-Moreux, C., 1993. Amphibian micronucleus test(s): a simple and reliable method for evaluating in vivo genotoxic effects of freshwater pollutants and radiations. Initial assessment. Mutation Research/Environmental Mutagenesis and Related Subjects 292, 83–99. https://doi.org/10.1016/0165-1161(93)90010-W
Fontaine, S.S., Mineo, P.M., Kohl, K.D., 2022. Experimental manipulation of microbiota reduces host thermal tolerance and fitness under heat stress in a vertebrate ectotherm. Nat Ecol Evol 1–13. https://doi.org/10.1038/s41559-022-01686-2
Freixa, A., Acuña, V., Sanchís, J., Farré, M., Barceló, D., Sabater, S., 2018. Ecotoxicological effects of carbon based nanomaterials in aquatic organisms. Science of The Total Environment 619–620, 328–337. https://doi.org/10.1016/j.scitotenv.2017.11.095
Gao, Y., Zeng, X., Zhang, W., Zhou, L., Xue, W., Tang, M., Sun, S., 2022. The aggregation behaviour and mechanism of commercial graphene oxide in surface aquatic environments. Science of The Total Environment 806, 150942. https://doi.org/10.1016/j.scitotenv.2021.150942
Gibiino, G., Lopetuso, L.R., Scaldaferri, F., Rizzatti, G., Binda, C., Gasbarrini, A., 2018. Exploring Bacteroidetes: Metabolic key points and immunological tricks of our gut commensals. Digestive and Liver Disease 50, 635–639. https://doi.org/10.1016/j.dld.2018.03.016
Goodwin, A.C., Destefano Shields, C.E., Wu, S., Huso, D.L., Wu, X., Murray-Stewart, T.R., Hacker-Prietz, A., Rabizadeh, S., Woster, P.M., Sears, C.L., Casero, R.A., 2011. Polyamine catabolism contributes to enterotoxigenic Bacteroides fragilis-induced colon tumorigenesis. Proc Natl Acad Sci U S A 108, 15354–15359. https://doi.org/10.1073/pnas.1010203108
Goodwin, D.G., Adeleye, A.S., Sung, L., Ho, K.T., Burgess, R.M., Petersen, E.J., 2018. Detection and quantification of Graphene-family nanomaterials in the environment. Environmental Science & Technology 52, 4491–4513. https://doi.org/10.1021/acs.est.7b04938
Gopinath, K.P., Vo, D.-V.N., Gnana Prakash, D., Adithya Joseph, A., Viswanathan, S., Arun, J., 2021. Environmental applications of carbon-based materials: a review. Environ Chem Lett 19, 557–582. https://doi.org/10.1007/s10311-020-01084-9
Guo, Z., Xie, C., Zhang, P., Zhang, J., Wang, G., He, X., Ma, Y., Zhao, B., Zhang, Z., 2017. Toxicity and transformation of graphene oxide and reduced graphene oxide in bacteria biofilm. Science of The Total Environment 580, 1300–1308. https://doi.org/10.1016/j.scitotenv.2016.12.093
Hegab, H.M., ElMekawy, A., Zou, L., Mulcahy, D., Saint, C.P., Ginic-Markovic, M., 2016. The controversial antibacterial activity of graphene-based materials. Carbon 105, 362–376. https://doi.org/10.1016/j.carbon.2016.04.046
Heimeier, R.A., Das, B., Buchholz, D.R., Fiorentino, M., Shi, Y.-B., 2010. Studies on Xenopus laevis intestine reveal biological pathways underlying vertebrate gut adaptation from embryo to adult. Genome Biol 11, R55. https://doi.org/10.1186/gb-2010-11-5-r55

753 Hu, X., Wei, Z., Mu, L., 2017. Graphene oxide nanosheets at trace concentrations elicit neurotoxicity in
754 the offspring of zebrafish. Carbon 117, 182–191.
755 https://doi.org/10.1016/j.carbon.2017.02.092
756 Hummers, W.S., Offeman, R.E., 1958. Preparation of Graphitic Oxide. J. Am. Chem. Soc. 80, 1339–1339.
757 https://doi.org/10.1021/ja01539a017
758 Jastrzębska, A.M., Olszyna, A.R., 2015. The ecotoxicity of graphene family materials: current status,
759 knowledge gaps and future needs. Journal of Nanoparticle Research 17, 40.
760 https://doi.org/10.1007/s11051-014-2817-0
761 Jia, P.-P., Sun, T., Junaid, M., Xiong, Y.-H., Wang, Y.-Q., Liu, L., Pu, S.-Y., Pei, D.-S., 2019. Chronic
762 exposure to graphene oxide (GO) induced inflammation and differentially disturbed the
763 intestinal microbiota in zebrafish. Environ. Sci.: Nano 6, 2452–2469.
764 https://doi.org/10.1039/C9EN00364A
765 Johra, F.T., Lee, J.-W., Jung, W.-G., 2014. Facile and safe graphene preparation on solution based
766 platform. Journal of Industrial and Engineering Chemistry 20, 2883–2887.
767 https://doi.org/10.1016/j.jiec.2013.11.022
768 Katoh, K., Misawa, K., Kuma, K., Miyata, T., 2002. MAFFT: a novel method for rapid multiple sequence
769 alignment based on fast Fourier transform. Nucleic Acids Res 30, 3059–3066.
770 https://doi.org/10.1093/nar/gkf436
771 Knutie, S.A., Gabor, C.R., Kohl, K.D., Rohr, J.R., 2018. Do host-associated gut microbiota mediate the
772 effect of an herbicide on disease risk in frogs? Journal of Animal Ecology 87, 489–499.
773 https://doi.org/10.1111/1365-2656.12769
774 Knutie, S.A., Shea, L.A., Kupselaitis, M., Wilkinson, C.L., Kohl, K.D., Rohr, J.R., 2017. Early-Life Diet
775 Affects Host Microbiota and Later-Life Defenses Against Parasites in Frogs. Integrative and
776 Comparative Biology 57, 732–742. https://doi.org/10.1093/icb/icx028
777 Koh, A., De Vadder, F., Kovatcheva-Datchary, P., Bäckhed, F., 2016. From Dietary Fiber to Host
778 Physiology: Short-Chain Fatty Acids as Key Bacterial Metabolites. Cell 165, 1332–1345.
779 https://doi.org/10.1016/j.cell.2016.05.041
780 Kohl, K.D., Amaya, J., Passement, C.A., Dearing, M.D., McCue, M.D., 2014. Unique and shared
781 responses of the gut microbiota to prolonged fasting: a comparative study across five classes
782 of vertebrate hosts. FEMS Microbiology Ecology 90, 883–894. https://doi.org/10.1111/1574-
783 6941.12442
784 Kohl, K.D., Cary, T.L., Karasov, W.H., Dearing, M.D., 2013. Restructuring of the amphibian gut
785 microbiota through metamorphosis: The amphibian gut microbiota. Environmental
786 Microbiology Reports 5, 899–903. https://doi.org/10.1111/1758-2229.12092
787 Krajmalnik-Brown, R., Ilhan, Z.-E., Kang, D.-W., DiBaise, J.K., 2012. Effects of Gut Microbes on Nutrient
788 Absorption and Energy Regulation. Nutrition in Clinical Practice 27, 201–214.
789 https://doi.org/10.1177/0884533611436116
790 Kumar, A., Sharma, K., Dixit, A.R., 2019. A review of the mechanical and thermal properties of graphene
791 and its hybrid polymer nanocomposites for structural applications. J Mater Sci 54, 5992–6026.
792 https://doi.org/10.1007/s10853-018-03244-3
793 Lagier, L., Mouchet, F., Laplanche, C., Mottier, A., Cadarsi, S., Evariste, L., Sarrieu, C., Lonchambon, P.,
794 Pinelli, E., Flahaut, E., Gauthier, L., 2017. Surface area of carbon-based nanoparticles prevails
795 on dispersion for growth inhibition in amphibians. Carbon 119, 72–81.
796 https://doi.org/10.1016/j.carbon.2017.04.016
797 Lee, W.-J., Hase, K., 2014. Gut microbiota–generated metabolites in animal health and disease. Nat
798 Chem Biol 10, 416–424. https://doi.org/10.1038/nchembio.1535
799 Ley, R.E., Peterson, D.A., Gordon, J.I., 2006a. Ecological and Evolutionary Forces Shaping Microbial
800 Diversity in the Human Intestine. Cell 124, 837–848.
801 https://doi.org/10.1016/j.cell.2006.02.017
802 Ley, R.E., Turnbaugh, P.J., Klein, S., Gordon, J.I., 2006b. Human gut microbes associated with obesity.
803 Nature 444, 1022.

Li, J., Yang, S., Yu, J., Cui, R., Liu, R., Lei, R., Chang, Y., Geng, H., Qin, Y., Gu, W., Xia, S., Chen, K., Kong, J., Chen, G., Wu, C., Xing, G., 2018. Lipid- and gut microbiota-modulating effects of graphene oxide nanoparticles in high-fat diet-induced hyperlipidemic mice. RSC Adv. 8, 31366–31371. https://doi.org/10.1039/C8RA06058D

Li, M., Zhu, J., Wang, M., Fang, H., Zhu, G., Wang, Q., 2019. Exposure to graphene oxide at environmental concentrations induces thyroid endocrine disruption and lipid metabolic disturbance in Xenopus laevis. Chemosphere 236, 124834. https://doi.org/10.1016/j.chemosphere.2019.124834

Lin, L., Peng, H., Liu, Z., 2019. Synthesis challenges for graphene industry. Nature Materials 18, 520–524. https://doi.org/10.1038/s41563-019-0341-4

Lin, X., Xu, Y., Han, R., Luo, W., Zheng, L., 2022. Migration of antibiotic resistance genes and evolution of flora structure in the Xenopus tropicalis intestinal tract with combined exposure to roxithromycin and oxytetracycline. Science of The Total Environment 820, 153176. https://doi.org/10.1016/j.scitotenv.2022.153176

Liu, J., Cui, L., Losic, D., 2013. Graphene and graphene oxide as new nanocarriers for drug delivery applications. Acta Biomaterialia 9, 9243–9257. https://doi.org/10.1016/j.actbio.2013.08.016

Liu, L., Zhu, C., Fan, M., Chen, C., Huang, Y., Hao, Q., Yang, J., Wang, H., Sun, D., 2015. Oxidation and degradation of graphitic materials by naphthalene-degrading bacteria. Nanoscale 7, 13619–13628. https://doi.org/10.1039/C5NR02502H

Liu, S., Zeng, T.H., Hofmann, M., Burcombe, E., Wei, J., Jiang, R., Kong, J., Chen, Y., 2011. Antibacterial activity of graphite, graphite oxide, graphene oxide, and reduced graphene oxide: Membrane and oxidative stress. ACS Nano 5, 6971–6980. https://doi.org/10.1021/nn202451x

Liu, X., Zhang, F., Wang, Zengjin, Zhang, T., Teng, C., Wang, Zhiping, 2021. Altered gut microbiome accompanying with placenta barrier dysfunction programs pregnant complications in mice caused by graphene oxide. Ecotoxicology and Environmental Safety 207, 111143. https://doi.org/10.1016/j.ecoenv.2020.111143

Lobato, B., Merino, C., Barranco, V., Centeno, T.A., 2016. Large-scale conversion of helical-ribbon carbon nanofibers to a variety of graphene-related materials. RSC Advances 6, 57514–57520. https://doi.org/10.1039/C6RA08865A

Lv, X., Yang, Y., Tao, Y., Jiang, Y., Chen, B., Zhu, X., Cai, Z., Li, B., 2018. A mechanism study on toxicity of graphene oxide to Daphnia magna: Direct link between bioaccumulation and oxidative stress. Environmental Pollution 234, 953–959. https://doi.org/10.1016/j.envpol.2017.12.034

Ma, K., Zhang, S., Ye, B., Ouyang, J., Yue, G.H., 2016. A new view of graphene oxide biosafety in a water environment using an eatable fish as a model. RSC Adv. 6, 29619–29623. https://doi.org/10.1039/C5RA26026D

McDonald, D., Price, M.N., Goodrich, J., Nawrocki, E.P., DeSantis, T.Z., Probst, A., Andersen, G.L., Knight, R., Hugenholtz, P., 2012. An improved Greengenes taxonomy with explicit ranks for ecological and evolutionary analyses of bacteria and archaea. ISME J 6, 610–618. https://doi.org/10.1038/ismej.2011.139

Mcgill, R., Tukey, J.W., Larsen, W.A., 1978. Variations of Box Plots. The American Statistician 32, 12–16. https://doi.org/10.1080/00031305.1978.10479236

Miclotte, L., De Paepe, K., Rymenans, L., Callewaert, C., Raes, J., Rajkovic, A., Van Camp, J., Van de Wiele, T., 2020. Dietary Emulsifiers Alter Composition and Activity of the Human Gut Microbiota in vitro, Irrespective of Chemical or Natural Emulsifier Origin. Frontiers in Microbiology 11.

Mohammed, H., Kumar, A., Bekyarova, E., Al-Hadeethi, Y., Zhang, X., Chen, M., Ansari, M.S., Cochis, A., Rimondini, L., 2020. Antimicrobial Mechanisms and Effectiveness of Graphene and Graphene-Functionalized Biomaterials. A Scope Review. Frontiers in Bioengineering and Biotechnology 8.

Montagner, A., Bosi, S., Tenori, E., Bidussi, M., Alshatwi, A.A., Tretiach, M., Prato, M., Syrgiannis, Z., 2016. Ecotoxicological effects of graphene-based materials. 2D Materials 4, 012001. https://doi.org/10.1088/2053-1583/4/1/012001

Mottier, A., Mouchet, F., Laplanche, C., Cadarsi, S., Lagier, L., Arnault, J.-C., Girard, H.A., León, V., Vázquez, E., Sarrieu, C., Pinelli, É., Gauthier, L., Flahaut, E., 2016. Surface Area of Carbon Nanoparticles: A Dose Metric for a More Realistic Ecotoxicological Assessment. Nano Letters 16, 3514–3518. https://doi.org/10.1021/acs.nanolett.6b00348

Mottier, A., Mouchet, F., Pinelli, É., Gauthier, L., Flahaut, E., 2017. Environmental impact of engineered carbon nanoparticles: from releases to effects on the aquatic biota. Current Opinion in Biotechnology 46, 1–6. https://doi.org/10.1016/j.copbio.2016.11.024

Nieuwkoop, P.D., Faber, J., 1958. Normal table of Xenopus laevis (Daudin). A systematical and chronological survey of the development from the fertilized egg till the end of metamorphosis. The Quarterly Review of Biology 33, 85–85. https://doi.org/10.1086/402265

Olabi, A.G., Abdelkareem, M.A., Wilberforce, T., Sayed, E.T., 2021. Application of graphene in energy storage device – A review. Renewable and Sustainable Energy Reviews 135, 110026. https://doi.org/10.1016/j.rser.2020.110026

Pantosti, A., Malpeli, M., Wilks, M., Menozzi, M.G., D'Ambrosio, F., 1997. Detection of enterotoxigenic Bacteroides fragilis by PCR. J Clin Microbiol 35, 2482–2486. https://doi.org/10.1128/jcm.35.10.2482-2486.1997

Peng, Z., Ehrmann, M.A., Waldhuber, A., Niemeyer, C., Miethke, T., Frick, J.-S., Xiong, T., Vogel, R.F., 2017. Phosphotransferase systems in Enterococcus faecalis OG1RF enhance anti-stress capacity in vitro and in vivo. Research in Microbiology 168, 558–566. https://doi.org/10.1016/j.resmic.2017.03.003

Perreault, F., Fonseca de Faria, A., Elimelech, M., 2015. Environmental applications of graphene-based nanomaterials. Chemical Society Reviews 44, 5861–5896. https://doi.org/10.1039/C5CS00021A

Price, M.N., Dehal, P.S., Arkin, A.P., 2009. FastTree: Computing Large Minimum Evolution Trees with Profiles instead of a Distance Matrix. Molecular Biology and Evolution 26, 1641–1650. https://doi.org/10.1093/molbev/msp077

Pryor, G.S., Bjorndal, K.A., 2005. Symbiotic fermentation, digesta passage, and gastrointestinal morphology in bullfrog tadpoles (Rana catesbeiana). Physiol Biochem Zool 78, 201–215. https://doi.org/10.1086/427050

Ranjan, R., Rani, A., Metwally, A., McGee, H.S., Perkins, D.L., 2016. Analysis of the microbiome: Advantages of whole genome shotgun versus 16S amplicon sequencing. Biochem Biophys Res Commun 469, 967–977. https://doi.org/10.1016/j.bbrc.2015.12.083

Ren, X., Li, J., Chen, C., Gao, Y., Chen, D., Su, M., Alsaedi, A., Hayat, T., 2018. Graphene analogues in aquatic environments and porous media: dispersion, aggregation, deposition and transformation. Environ. Sci.: Nano 5, 1298–1340. https://doi.org/10.1039/C7EN01258F

Ruiz, O.N., Fernando, K.A.S., Wang, B., Brown, N.A., Luo, P.G., McNamara, N.D., Vangsness, M., Sun, Y.-P., Bunker, C.E., 2011. Graphene Oxide: A nonspecific enhancer of cellular growth. ACS Nano 5, 8100–8107. https://doi.org/10.1021/nn202699t

Saxena, P., Sangela, V., Ranjan, S., Dutta, V., Dasgupta, N., Phulwaria, M., Rathore, D.S., Harish, 2020. Aquatic nanotoxicology: impact of carbon nanomaterials on algal flora. Energ. Ecol. Environ. 5, 240–252. https://doi.org/10.1007/s40974-020-00151-9

Scalvenzi, T., Clavereau, I., Bourge, M., Pollet, N., 2021. Gut microbial ecology of Xenopus tadpoles across life stages. https://doi.org/10.1101/2020.05.25.110734

Schreiber, A.M., Cai, L., Brown, D.D., 2005. Remodeling of the intestine during metamorphosis of Xenopus laevis. PNAS 102, 3720–3725. https://doi.org/10.1073/pnas.0409868102

Scott, D.E., Casey, E.D., Donovan, M.F., Lynch, T.K., 2007. Amphibian lipid levels at metamorphosis correlate to post-metamorphic terrestrial survival. Oecologia 153, 521–532. https://doi.org/10.1007/s00442-007-0755-6

Scown, T.M., van Aerle, R., Tyler, C.R., 2010. Review: Do engineered nanoparticles pose a significant threat to the aquatic environment? Critical Reviews in Toxicology 40, 653–670. https://doi.org/10.3109/10408444.2010.494174

907 Segata, N., Izard, J., Waldron, L., Gevers, D., Miropolsky, L., Garrett, W.S., Huttenhower, C., 2011.
908 Metagenomic biomarker discovery and explanation. Genome Biology 12, R60.
909 https://doi.org/10.1186/gb-2011-12-6-r60
910 Sehnal, L., Brammer-Robbins, E., Wormington, A.M., Blaha, L., Bisesi, J., Larkin, I., Martyniuk, C.J.,
911 Simonin, M., Adamovsky, O., 2021. Microbiome Composition and Function in Aquatic
912 Vertebrates: Small Organisms Making Big Impacts on Aquatic Animal Health. Frontiers in
913 Microbiology 12.
914 Sengupta, I., Bhattacharya, P., Talukdar, M., Neogi, S., Pal, S.K., Chakraborty, S., 2019. Bactericidal
915 effect of graphene oxide and reduced graphene oxide: Influence of shape of bacteria. Colloid
916 and Interface Science Communications 28, 60–68.
917 https://doi.org/10.1016/j.colcom.2018.12.001
918 Shi, Y.-B., Fu, L., Hsia, S.C.V., Tomita, A., Buchholz, D., 2001. Thyroid hormone regulation of apoptotic
919 tissue remodeling during anuran metamorphosis. Cell Res 11, 245–252.
920 https://doi.org/10.1038/sj.cr.7290093
921 Souza, J.P., Baretta, J.F., Santos, F., Paino, I.M.M., Zucolotto, V., 2017. Toxicological effects of graphene
922 oxide on adult zebrafish (Danio rerio). Aquatic Toxicology 186, 11–18.
923 https://doi.org/10.1016/j.aquatox.2017.02.017
924 Souza, J.P., Venturini, F.P., Santos, F., Zucolotto, V., 2018. Chronic toxicity in Ceriodaphnia dubia
925 induced by graphene oxide. Chemosphere 190, 218–224.
926 https://doi.org/10.1016/j.chemosphere.2017.10.018
927 Sterling, J., Fu, L., Matsuura, K., Shi, Y.-B., 2012. Cytological and Morphological Analyses Reveal Distinct
928 Features of Intestinal Development during Xenopus tropicalis Metamorphosis. PLOS ONE 7,
929 e47407. https://doi.org/10.1371/journal.pone.0047407
930 Sun, S., Jones, R.B., Fodor, A.A., 2020. Inference-based accuracy of metagenome prediction tools varies
931 across sample types and functional categories. Microbiome 8, 46.
932 https://doi.org/10.1186/s40168-020-00815-y
933 Sun, T.Y., Bornhöft, N.A., Hungerbühler, K., Nowack, B., 2016. Dynamic Probabilistic Modeling of
934 Environmental Emissions of Engineered Nanomaterials. Environ. Sci. Technol. 50, 4701–4711.
935 https://doi.org/10.1021/acs.est.5b05828
936 Suter, J.L., Coveney, P.V., 2021. Principles governing control of aggregation and dispersion of aqueous
937 graphene oxide. Sci Rep 11, 22460. https://doi.org/10.1038/s41598-021-01626-3
938 Székely, D., Cogălniceanu, D., Székely, P., Armijos-Ojeda, D., Espinosa-Mogrovejo, V., Denoël, M., 2020.
939 How to recover from a bad start: size at metamorphosis affects growth and survival in a
940 tropical amphibian. BMC Ecology 20, 24. https://doi.org/10.1186/s12898-020-00291-w
941 Tashan, H., Khosravi-Darani, K., Yazdian, F., Omidi, M., Sheikhpour, M., Farahani, M., Omri, A., 2019.
942 Antibacterial Properties of Graphene Based Nanomaterials: An Emphasis on Molecular
943 Mechanisms, Surface Engineering and Size of Sheets. Mini-Reviews in Organic Chemistry 16,
944 159–172. https://doi.org/10.2174/1570193X15666180712120309
945 Tegou, E., Magana, M., Katsogridaki, A.E., Ioannidis, A., Raptis, V., Jordan, S., Chatzipanagiotou, S.,
946 Chatzandroulis, S., Ornelas, C., Tegos, G.P., 2016. Terms of endearment: Bacteria meet
947 graphene nanosurfaces. Biomaterials 89, 38–55.
948 https://doi.org/10.1016/j.biomaterials.2016.02.030
949 Wang, Y., Qian, P.-Y., 2009. Conservative fragments in bacterial 16S rRNA genes and primer design for
950 16S Ribosomal DNA amplicons in metagenomic studies. PLOS ONE 4, e7401.
951 https://doi.org/10.1371/journal.pone.0007401
952 Wiles, T.J., Schlomann, B.H., Wall, E.S., Betancourt, R., Parthasarathy, R., Guillemin, K., 2020. Swimming
953 motility of a gut bacterial symbiont promotes resistance to intestinal expulsion and enhances
954 inflammation. PLOS Biology 18, e3000661. https://doi.org/10.1371/journal.pbio.3000661
955 Woting, A., Blaut, M., 2016. The Intestinal Microbiota in Metabolic Disease. Nutrients 8, 202.
956 https://doi.org/10.3390/nu8040202
957 Xie, Y., Wu, B., Zhang, X.-X., Yin, J., Mao, L., Hu, M., 2016. Influences of graphene on microbial
958 community and antibiotic resistance genes in mouse gut as determined by high-throughput

sequencing. Chemosphere 144, 1306–1312. https://doi.org/10.1016/j.chemosphere.2015.09.076
Yin, J., Fan, W., Du, J., Feng, W., Dong, Z., Liu, Y., Zhou, T., 2020. The toxicity of graphene oxide affected by algal physiological characteristics: A comparative study in cyanobacterial, green algae, diatom. Environmental Pollution 260, 113847. https://doi.org/10.1016/j.envpol.2019.113847
Zhang, C., Wang, Y., Zhao, H., 2020. Is Graphene Oxide a Chemoattractant? Nano Lett. 20, 1455–1460. https://doi.org/10.1021/acs.nanolett.9b05234
Zhang, J., Wang, Z., Wang, Y., Zhong, H., Sui, Q., Zhang, C., Wei, Y., 2017. Effects of graphene oxide on the performance, microbial community dynamics and antibiotic resistance genes reduction during anaerobic digestion of swine manure. Bioresource Technology 245, 850–859. https://doi.org/10.1016/j.biortech.2017.08.217
Zhang, T., Zhu, G.-Y., Yu, C.-H., Xie, Y., Xia, M.-Y., Lu, B.-Y., Fei, X., Peng, Q., 2019. The UV absorption of graphene oxide is size-dependent: possible calibration pitfalls. Mikrochim Acta 186, 207. https://doi.org/10.1007/s00604-019-3329-5
Zheng, M., Lu, J., Lin, G., Su, H., Sun, J., Luan, T., 2019. Dysbiosis of gut microbiota by dietary exposure of three graphene-family materials in zebrafish (Danio rerio). Environ Pollut 254, 112969. https://doi.org/10.1016/j.envpol.2019.112969
Zhu, W., Chang, L., Shu, G., Wang, B., Jiang, J., 2021. Fatter or stronger: Resource allocation strategy and the underlying metabolic mechanisms in amphibian tadpoles. Comparative Biochemistry and Physiology Part D: Genomics and Proteomics 38, 100825. https://doi.org/10.1016/j.cbd.2021.100825
Zhu, W., Chang, L., Zhao, T., Wang, B., Jiang, J., 2020. Remarkable metabolic reorganization and altered metabolic requirements in frog metamorphic climax. Frontiers in Zoology 17, 30. https://doi.org/10.1186/s12983-020-00378-6
Zhu, Wei, Zhang, M., Chang, L., Zhu, Wenbo, Li, C., Xie, F., Zhang, H., Zhao, T., Jiang, J., 2019. Characterizing the composition, metabolism and physiological functions of the fatty liver in Rana omeimontis tadpoles. Frontiers in Zoology 16, 42. https://doi.org/10.1186/s12983-019-0341-x
Zhu, Y., Ji, H., Cheng, H.-M., Ruoff, R.S., 2018. Mass production and industrial applications of graphene materials. National Science Review 5, 90–101. https://doi.org/10.1093/nsr/nwx055
Zou, X., Zhang, L., Wang, Z., Luo, Y., 2016. Mechanisms of the Antimicrobial Activities of Graphene Materials. J. Am. Chem. Soc. 138, 2064–2077. https://doi.org/10.1021/jacs.5b11411

Table

Table 1: Physico-chemical characteristics of GO used for the experiment. at. %: atomic %; TEM: transmission electron microscope; HRTEM: high resolution TEM; BET: Brunauer-Emett-Teller.

	Graphene Oxide
Carbon content	69.1 ± 0.4 at. %
Oxygen content	31.1 ± 0.4 at. %
Number of layers (HRTEM)	1–5
Lateral size (TEM)	0.2 to 8 µm
Specific surface area (BET)	228 ± 6.8 $m^2.g^{-1}$

Table 2: *X. laevis* erythrocyte cell cycle distribution analyzed using flow cytometry after 12 days of exposure to increasing GO concentrations. Letters indicate significant differences between groups.

	GO/G1 (% cells)	**S (% cells)**	**G2/M (% cells)**
Control	77.69 ± 0.86 **A**	11.11 ± 0.27 **AB**	11,2 ± 0.86 **A**
0.05 mg/L	84.72 ± 0.83 **B**	6.49 ± 0.15 **C**	8.79 ± 0.80 **AB**
0.1 mg/L	80.02 ± 0.45 **C**	10.43 ± 0.35 **B**	9.55 ± 0.32 **AB**
1 mg/L	83.92 ± 0.42 **B**	8.60 ± 0.25 **D**	7.47 ± 0.33 **B**
10 mg/L	79.81 ± 0.56 **AC**	11.57 ± 0.25 **A**	8.62 ± 0.48 **B**

Figure captions

Figure 1: Monitoring of the GO dispersion stability at 10 mg/L in the exposure media. Calibration plot based on optical density at 235 nm of increasing GO concentrations in exposure media (A). Dispersion stability kinetic in presence and absence of *X. laevis* tadpoles in the media (B). Area under the curve (AUC) in arbitrary unit was used to evaluate statistical differences of dispersion stability. *** indicate significant differences following T-test when p-value < 0.001.

Figure 2: Effects of GO exposure on *X. laevis* tadpole growth and intestinal developments. Larval growth rate monitored over the 12 days of exposure (A). Normalized growth rate determined after 2 (B) or 12 (C) days of exposure to increasing GO concentrations. Pictures of GO intestinal accumulation after 2 or 12 days of exposure (D). Intestinal weight measured after 2 (E) or 12 days of exposure. Letters indicate significant differences between concentrations determined by the post-hoc Tukey test when ANOVA p-value < 0.05.

Figure 3: Effects of an exposure to increasing GO concentrations on the abundance of intestinal bacteria as detected by qPCR. Evolution of intestinal bacterial load in the control group over time (A). Gut bacteria abundance measured after 2 (B) or 12 (C) days of exposure to increasing GO concentrations. Differences across groups were tested using ANOVA followed by post-hoc Tukey test when p-value < 0.05. Letters indicate significant differences between groups.

Figure 4: Effects of two days of exposure to increasing GO concentration on *X. laevis* tadpole's gut microbiota structure. Gut Microbiota richness (A) and evenness (B). PCoA plot of the bacterial communities based on Bray-Curtis dissimilarities (C). Comparison of the Bray-Curtis distances among experimental groups (D). Relative abundances of the phyla composing the gut microbiota of control or exposed larvae (E), including Bacteroidetes (F), Firmicutes (G), Proteobacteria (H) and Fusobacteria (I).

Differences across groups were tested using ANOVA followed by post-hoc Tukey test when p-value < 0.05. Letters indicate significant differences between groups (n = 5 per group).

Figure 5: Effects of 12 days of exposure to increasing GO towards gut bacterial communities of *X. laevis* tadpoles. Effects on alpha-diversity parameters measured using Richness (A) and Shannon Index (B). PCoA plot of the bacterial communities based on Bray-Curtis dissimilarities (C). Comparison of the Bray-Curtis distances among experimental groups (D). Effects of GO exposure on the main phyla relative abundances (E), including Bacteroidetes (F), Firmicutes (G), Proteobacteria (H) and Fusobacteria (I) and resulting Firmicutes/Bacteroidetes ratio (J). Relative abundances of the bacteria *Bacteroides fragilis* and bacteria from the genus Parabacteroides are represented based on the results from the LEfSe analysis (K). Differences across groups were tested using ANOVA followed by post-hoc Tukey test when p-value < 0.05. Letters indicate significant differences between groups (n = 5 per group).

Figure 6: Determination of taxa differentially abundant in the gut microbiome of larvae exposed during 12 days to GO compared to the control group characterized by LEfSe analysis. LDA score of taxa differentially abundant in larvae exposed to GO at 0.05 mg/L (A), 0.1 mg/L (B) and 10 mg/L (C). Cladogram representation of results from the LEfSe analysis following exposure to GO at 10 mg/L compared to the control.

Figure 7: Relation between gut microbiota alterations following 12 days of exposure to increasing GO concentration and genotoxic effects towards the host. Relative abundance of the bacteria *Bacteroides fragilis* in the gut at T12 (A). Micronucleated cells accounted in the host circulating erythrocytes (B). Correlation between micronucleus frequency and *B. fragilis* relative abundance (C). Letters indicate

significant differences between groups using post-hoc Tukey test. * indicate significant differences compared to the control group.

Figure_1

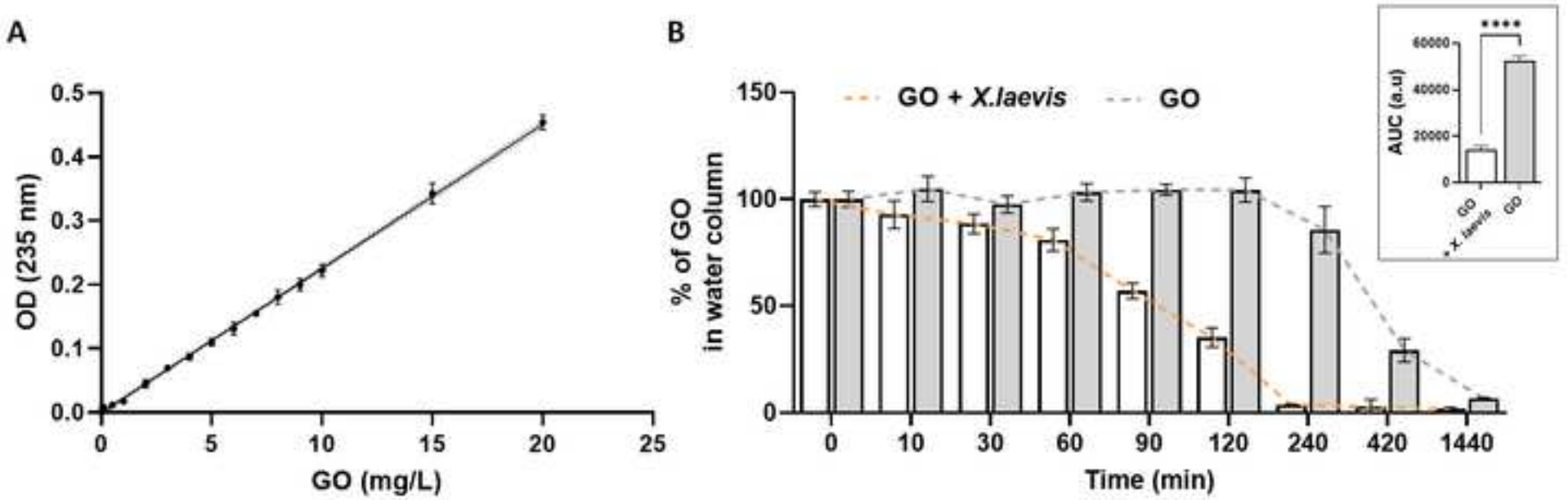

Figure_1 new.tif

Figure_2

Figure_1.tif

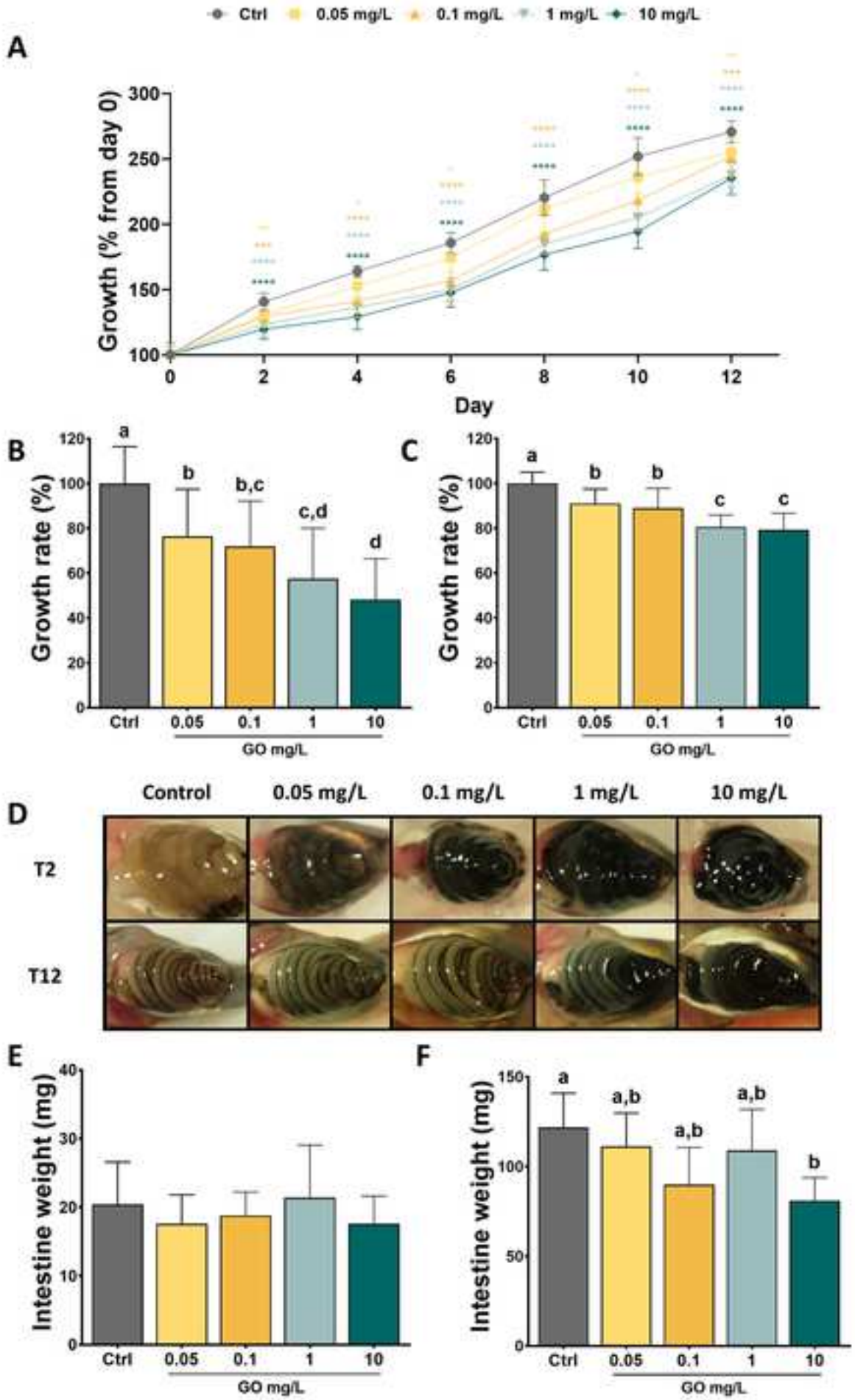

Figure_3

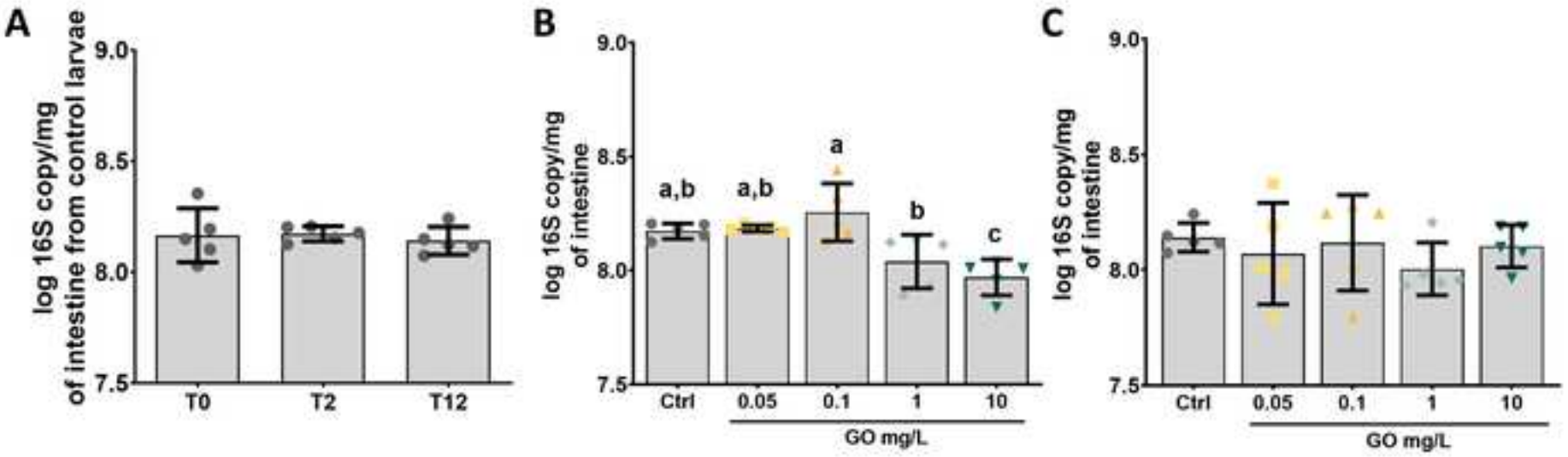

Figure_2.tif

Figure_4

Figure_3.tif

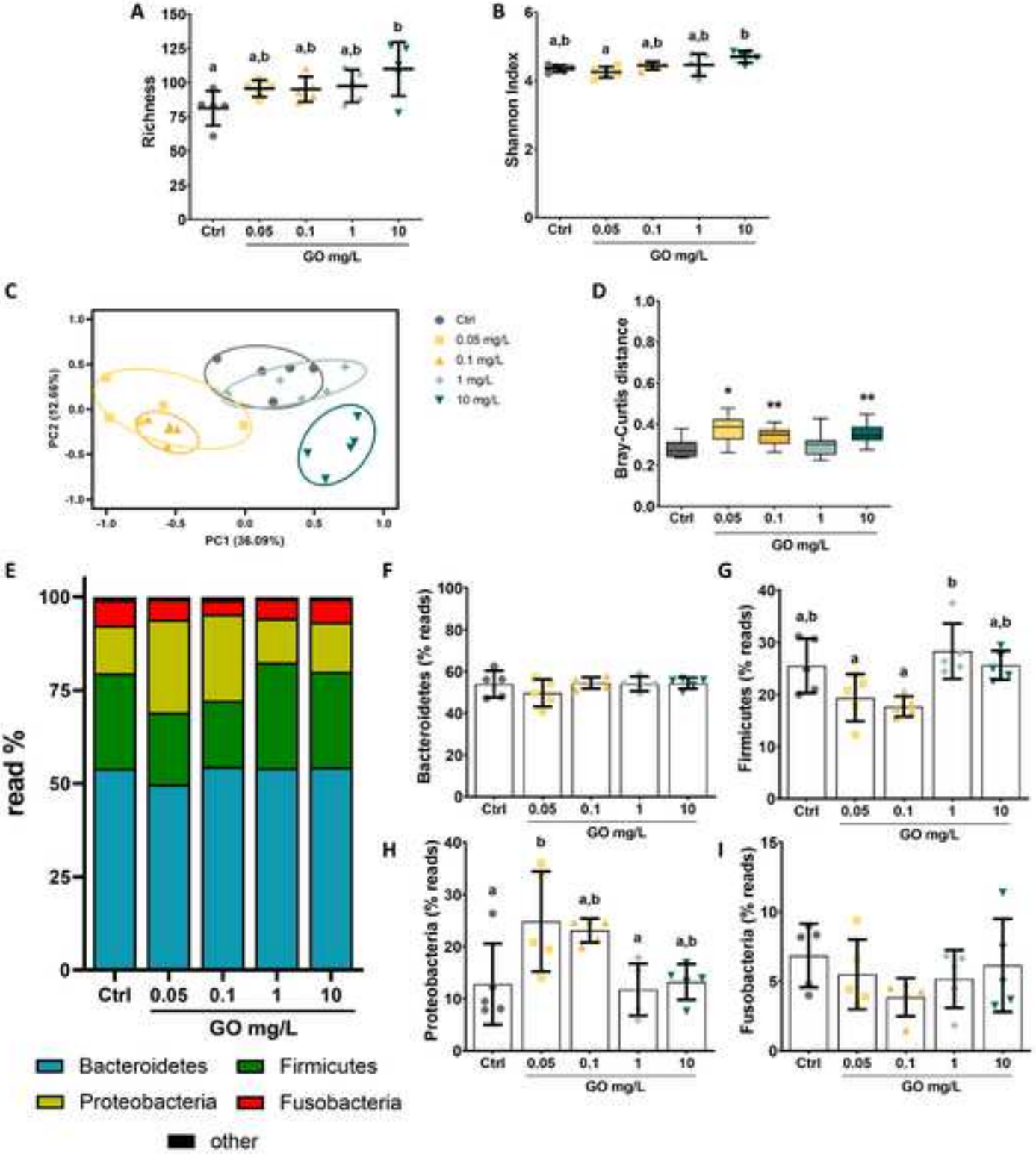

Figure_5

Figure_4.tif

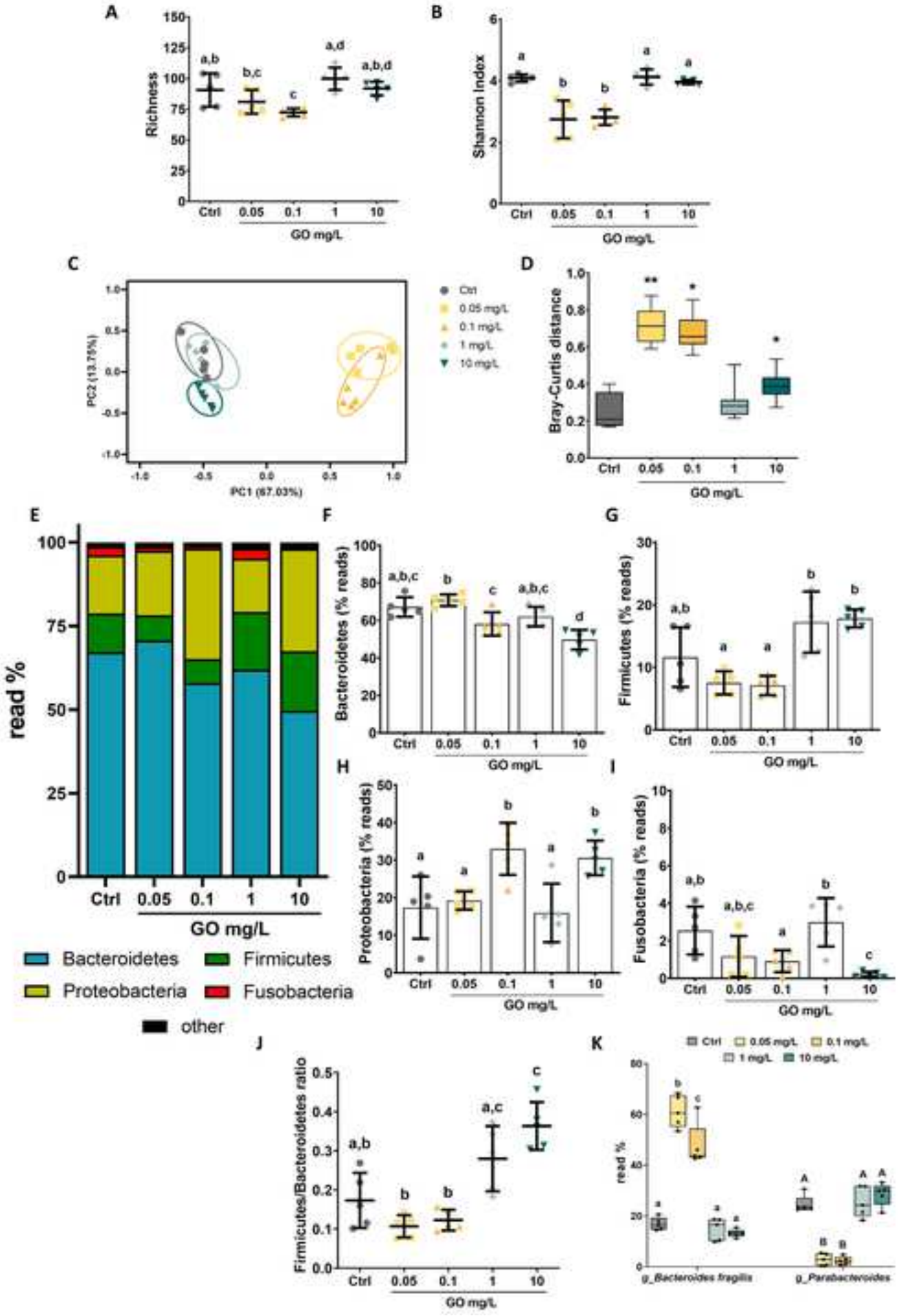

Figure_6

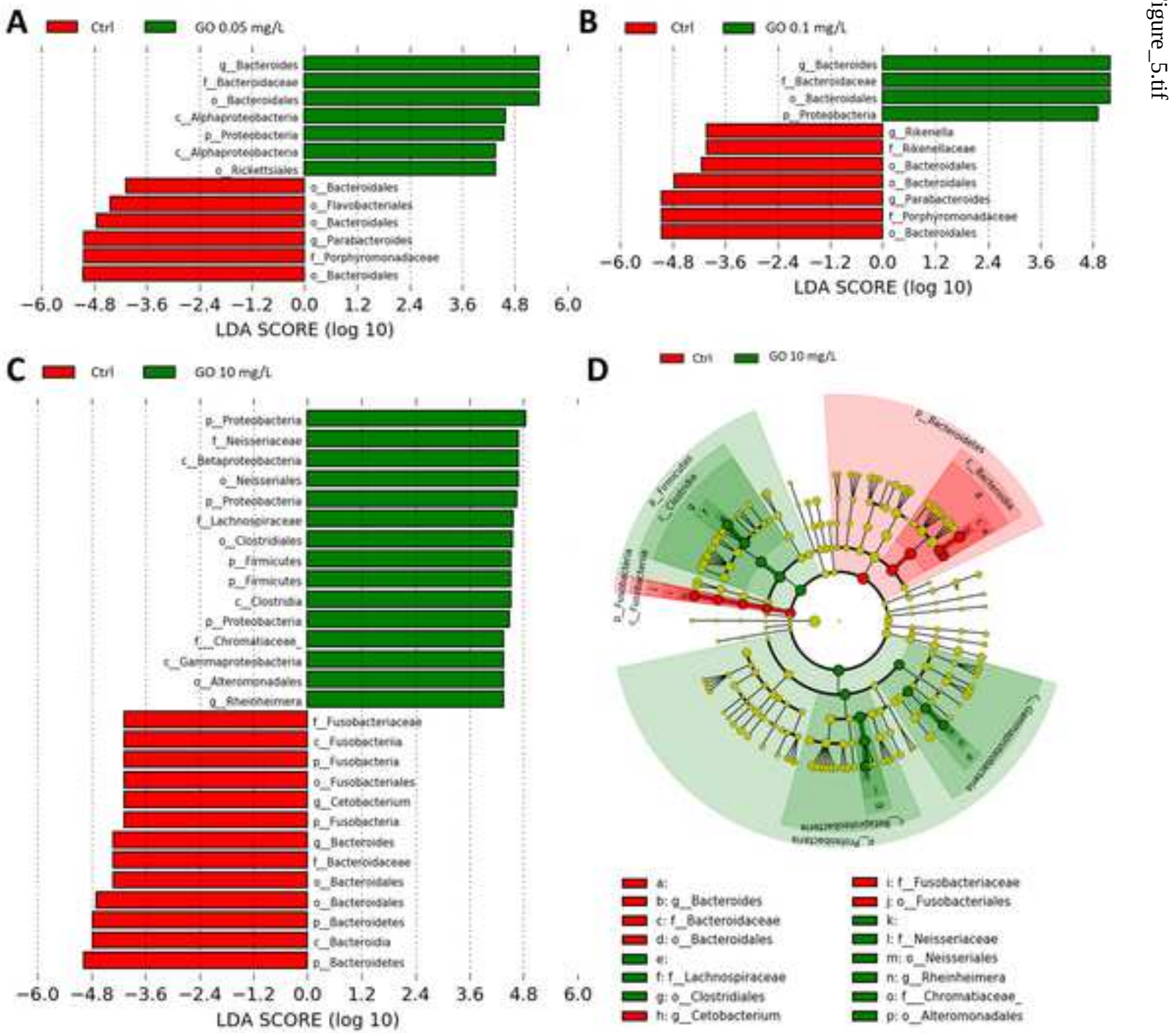

Figure_5.tif

Figure_7

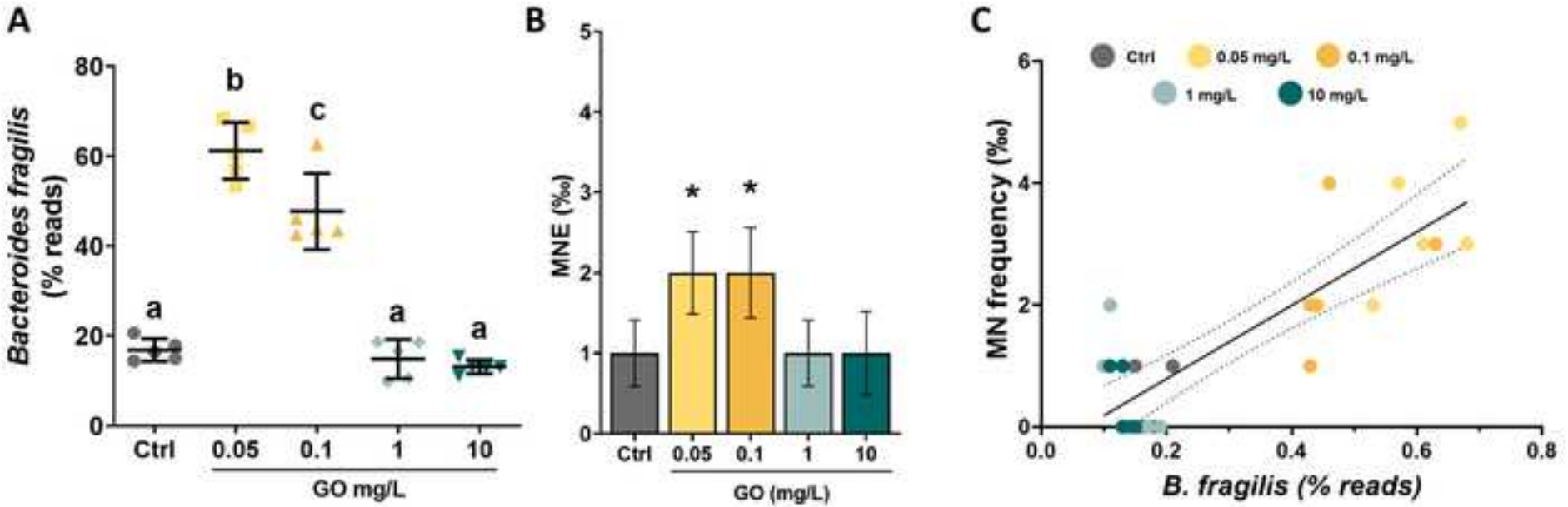

Figure_6.tif